

# Complexity of Higher-Degree Orthogonal Graph Embedding in the Kandinsky Model

Thomas Bläsius\*    Guido Brückner\*    Ignaz Rutter†

## Abstract

We show that finding orthogonal grid-embeddings of plane graphs (planar with fixed combinatorial embedding) with the minimum number of bends in the so-called Kandinsky model (which allows vertices of degree  $> 4$ ) is NP-complete, thus solving a long-standing open problem. On the positive side, we give an efficient algorithm for several restricted variants, such as graphs of bounded branch width and a subexponential exact algorithm for general plane graphs.

## 1 Introduction

Orthogonal grid embeddings are a fundamental topic in computer science and the problem of finding suitable grid embeddings of planar graphs is a subproblem in many applications, such as graph visualization [20] and VLSI design [17, 22]. Aside from the area requirement, the typical optimization goal is to minimize the number of bends on the edges (which also heuristically minimizes the area). Traditionally, grid embeddings have been studied for graphs with maximum degree 4, which is natural since it allows to represent vertices by grid points and edges by internally disjoint chains of horizontal and vertical segments on the grid. For a fixed combinatorial embedding Tamassia showed that the number of bends in the grid embedding can be efficiently minimized [14]; the running time was recently reduced to  $O(n^{1.5})$  [6]. In contrast, if the combinatorial embedding is not fixed, it is NP-complete to decide whether a 0-embedding (a *k-embedding* is a planar orthogonal grid embedding with at most  $k$  bends per edge) exists [14], thus also showing that bend minimization is NP-complete and hard to approximate within a factor of  $O(n^{1-\varepsilon})$ . In contrast, a 2-embedding exists for every graph except the octahedron [2]. Recently it was shown that the existence of a 1-embedding can be tested efficiently [3]. The problem is FPT if some subset of size  $k$  has to have 0 bends [4]. If there are no 0-bend edges, it

---

\*Faculty of Informatics, Karlsruhe Institute of Technology, Karlsruhe, [blaesius@kit.edu](mailto:blaesius@kit.edu), [guido.brueckner@student.kit.edu](mailto:guido.brueckner@student.kit.edu)

†Faculty of Informatics, Karlsruhe Institute of Technology, Karlsruhe and Department of Applied Mathematics, Faculty of Mathematics and Physics, Charles University, Prague, [rutter@kit.edu](mailto:rutter@kit.edu)

is even possible to minimize the number of bends in the embedding, where the first bend on each edge is not counted [5].

The main drawback of all these results is that they only apply to graphs of maximum degree 4. There have been several suggestions for possible generalizations to allow vertices of higher degree [16, 21]. For example, it is possible to model higher-degree vertices by boxes whose shape is restricted to a rectangle. The disadvantage is that, in this way, the vertices may be stretched arbitrarily in order to avoid bends. In particular, a visibility representation of a graph can be interpreted as a 0-embedding in this model (and such a representation exists for every planar graph). It is thus natural to forbid stretching of vertices.

Fößmeier and Kaufmann [13] proposed a generalization of planar orthogonal grid embeddings, the so-called Kandinsky model (originally called *podevsnef*), that overcomes this problem and guarantees that vertices are represented by boxes of uniform size. Essentially their model allows to map vertices to grid points on a coarse grid, while routing the edges on a much finer grid. The vertices are then interpreted as boxes on the finer grid, thus allowing several edges to emanate from the same side of a vertex; see Section 2 for a precise definition. Fößmeier and Kaufmann model the bend minimization in the fixed combinatorial embedding setting by a flow network similar to the work of Tamassia [19] but with additional constraints that limit the total amount of flow on some pairs of edges. Fößmeier et al. [12] later showed that every planar graph admits a 1-embedding in this model. Concerning bend minimization, reductions of the mentioned flow networks to ordinary minimum cost flows have been claimed both for general bend minimization [13] and for bend minimization when every edge may have at most one bend [12].

However, Eiglsperger [9] pointed out that the reductions to minimum cost flow is flawed and gave an efficient 2-approximation. Bertolazzi et al. [1] introduced a restricted variant of the Kandinsky model (which in general requires more bends), for which bend minimization can be done in polynomial time. Although the Kandinsky model has been later vastly generalized, e.g., to apply to the layout of UML class diagrams [10], the fundamental question about the complexity of the bend minimization problem in the Kandinsky model has remained open for almost two decades.

**Contribution and Outline.** In this work, we show that the bend minimization problem in the Kandinsky model is NP-complete even for graphs with a fixed combinatorial embedding (no matter if we allow or forbid so called empty faces). This also holds if each edge may have at most one bend; see Section 3. As an intermediate step, we show NP-hardness of the problem `ORTHOGONAL 01-EMBEDDABILITY`, which asks whether a plane graph (with maximum degree 4) admits a grid embedding when requiring some edges to have exactly one and the remaining edges to have zero bends. This is an interesting result on its own, as it can serve as tool to show hardness of other grid embedding problems. In particular, it gives a simpler proof for the hardness of deciding 0-embeddability in classic grid embeddings for graphs with a variable combinatorial embedding.

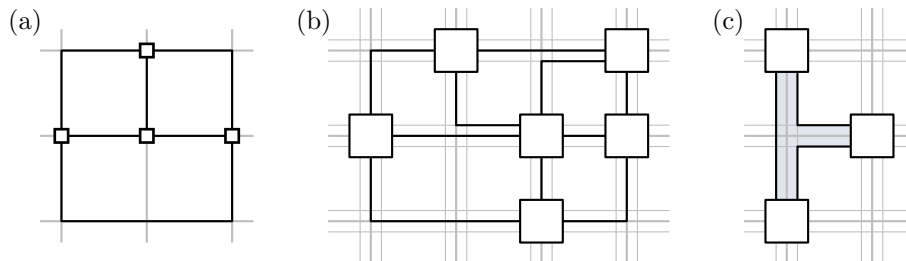


Figure 1: (a) An orthogonal embedding of the  $K_4$ . (b) A Kandinsky embedding of the wheel of size 5. (c) A Kandinsky embedding with an empty face.

We then study the complexity of the problem subject to structural graph parameters in Section 4. For graphs with branch width  $k$ , we obtain an algorithm with running time  $2^{O(k \log n)}$ . For fixed branch width this yields a polynomial-time algorithm (running time  $O(n^3)$  for series-parallel graphs), for general plane graphs the result is an exact algorithm with subexponential running time  $2^{O(\sqrt{n} \log n)}$ .

## 2 Preliminaries

The graphs we consider are always *plane*, i.e., they are planar and have a fixed combinatorial embedding. A planar graph is 4-planar if it has maximum degree 4. It is 4-plane, if it has a fixed combinatorial embedding.

### 2.1 Kandinsky Embedding

Let  $G$  be a plane graph. An *orthogonal embedding* of  $G$  maps each vertex to a grid point and each edge to a path in the grid such that the resulting drawing is planar and respects the combinatorial embedding of  $G$ ; see Figure 1a for an example. Clearly,  $G$  admits an orthogonal embedding if and only if no vertex has degree larger than 4. The Kandinsky model introduced by Fößmeier and Kaufmann [13] is a way to overcome this limitation. A *Kandinsky embedding* of  $G$  maps each vertex to a box of constant size centered at a grid point and each edge to a path in a finer grid such that the resulting drawing is planar and respects the combinatorial embedding of  $G$ ; see Figure 1b for an example. In a Kandinsky embedding, a face is *empty* if it does not include a grid cell of the coarser grid; see Figure 1c. Empty faces are empty in the sense that there is not enough space to add a vertex inside. Usually, one forbids empty faces in Kandinsky embeddings as allowing empty faces requires a special treatment for faces of size 3 compared to larger faces and cycles that are no faces. In the following, we always assume that empty faces are forbidden except when explicitly allowing them.

Every Kandinsky embedding has the so called *bend-or-end property*, which can be stated as follows. One can declare a bend on an edge  $e = uv$  to be *close*

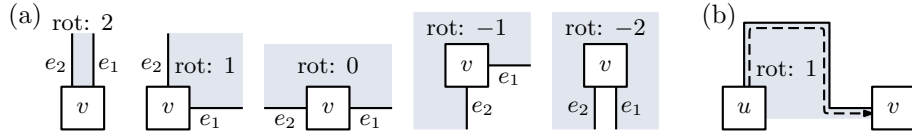


Figure 2: (a) The possible rotations at a vertex in the face  $f$  (shaded blue). (b) The rotation of an edge.

to  $v$  if it is the first bend when traversing  $e$  from  $v$  to  $u$  with the additional requirement that a bend cannot be close to both endpoints  $u$  and  $v$ . The bend-or-end property requires that an angle of  $0^\circ$  between edges  $uv$  and  $vw$  in the face  $f$  implies that at least one of the edges  $uv$  and  $vw$  has a bend close to  $v$  that is concave in  $f$  ( $270^\circ$  angle). Note that the triangle in Figure 1c does not have this property as the two concave bends cannot be close to all three vertices with  $0^\circ$  angles.

## 2.2 Kandinsky Representation

A Kandinsky embedding of a planar graph  $G$  can be specified in three stages. First, its topology is fixed by choosing a combinatorial embedding of  $G$  (which we assume to get with the input). Second, its shape in terms of angles between edges and sequences of bends on edges is fixed. Third, the geometry is fixed by specifying integer coordinates for all vertices and bend points. In analogy to the definition of combinatorial embeddings as equivalence classes of planar drawings with the same topology, one can define *Kandinsky representations* as equivalence classes of Kandinsky embeddings with the same topology and the same shape. As the number of bends (and thus the cost of an embedding) depends only on the shape and not on the geometry, we can focus on finding Kandinsky representations and thus neglect the geometry (at least if we make sure that every Kandinsky representation has a geometric realization as a Kandinsky embedding). For orthogonal embeddings, this approach was introduced by Tamassia [19]. It was extended to Kandinsky embeddings by Föbmeier and Kaufmann [13].

Let  $G$  be a planar graph with the Kandinsky embedding  $\Gamma$ . Let  $f$  be a face with the edge  $e_1$  in its boundary and let  $e_2$  be the successor of  $e_1$  in clockwise direction (counter-clockwise if  $f$  is the outer face). Let further  $v$  be the vertex between  $e_1$  and  $e_2$  and let  $\alpha$  be the angle at  $v$  in  $f$ . We define the *rotation*  $\text{rot}_f(e_1, e_2)$  between  $e_1$  and  $e_2$  to be  $\text{rot}_f(e_1, e_2) = 2 - \alpha/90^\circ$ ; see Figure 2a. The rotation  $\text{rot}_f(e_1, e_2)$  can be interpreted as the number of right turns between the edges  $e_1$  and  $e_2$  at the vertex  $v$  in the face  $f$ . Note that  $e_1 = e_2$  if  $v$  has degree 1, which yields  $\text{rot}_f(e_1, e_2) = -2$ . In case it is clear from the context which two edges are meant when referring to the vertex  $v$  in the face  $f$ , we also write  $\text{rot}_f(v)$  instead of  $\text{rot}_f(e_1, e_2)$  and call it the *rotation of  $v$  in  $f$* .

The shape of every edge can also be described in terms of its rotation. Let  $u$  be a vertex in the boundary of the face  $f$  and let  $v$  be its successor in clockwise

direction (counter-clockwise if  $f$  is the outer face). Let further  $e = uv$  be the corresponding edge. The *rotation*  $\text{rot}_f(e)$  of  $e$  in  $f$  is the number of right bends minus the number of left bends one encounters, when traversing  $e$  from  $u$  to  $v$ ; see Figure 2b. Note that every edge has two rotations, one in each face it bounds. Note further, that our notation is not precise for bridges, as a bridge is incident to the same face twice. However, it will always be clear from the context which incidence is meant, hence there is no need to complicate the notation.

Let  $uv, vw$  be a path of length 2 in the face  $f$ . If the two edges form an angle of  $0^\circ$  (i.e.,  $\text{rot}_f(v) = 2$ ), the bend-or-end property of Kandinsky drawings ensures that at least one of the two edges  $uv$  or  $vw$  has a bend close to  $v$  that forms an angle of  $270^\circ$  in  $f$ . To represent this information of which bends are declared to be close to vertices we introduce some additional rotations. Consider the edge  $uv$  and let  $f$  be an incident face. If  $uv$  has a bend close to  $v$  we define the *rotation*  $\text{rot}_f(uv[v])$  at the end  $v$  of  $uv$  to be 1 if it is a right bend and  $-1$  if it is a left bend. If  $uv$  has no bend close to  $v$ , we set  $\text{rot}_f(uv[v]) = 0$ .

It is easy to see, that every Kandinsky representation satisfies the following properties. Moreover, it is known that a set of values for the rotations is a Kandinsky representation if it satisfies these properties [13] (i.e., there exists a Kandinsky embedding with these rotation values).

- (1) The sum over all rotations in a face is 4 ( $-4$  for the outer face).
- (2) For every edge  $uv$  with incident face  $f_\ell$  and  $f_r$ , we have  $\text{rot}_{f_\ell}(uv) + \text{rot}_{f_r}(uv) = 0$ ,  $\text{rot}_{f_\ell}(uv[u]) + \text{rot}_{f_r}(uv[u]) = 0$ , and  $\text{rot}_{f_\ell}(uv[v]) + \text{rot}_{f_r}(uv[v]) = 0$ .
- (3) The sum of rotations around a vertex  $v$  is  $2 \cdot \deg(v) - 4$ .
- (4) The rotations at vertices lie in the range  $[-2, 2]$ .
- (5) If  $\text{rot}_f(uv, vw) = 2$  then  $\text{rot}_f(uv[v]) = -1$  or  $\text{rot}_f(vw[v]) = -1$ .

If the face is clear from the context, we often omit the subscript in  $\text{rot}_f$ . Note that the rotation of an edge  $uv$  is split into three parts; the rotations  $\text{rot}(uv[u])$  and  $\text{rot}(uv[v])$  at the ends of  $uv$  and a *rotation*  $\text{rot}(uv[-])$  in the center of  $uv$ . It holds  $\text{rot}(uv) = \text{rot}(uv[u]) + \text{rot}(uv[-]) + \text{rot}(uv[v])$  (thus it is not necessary to have  $\text{rot}(uv[-])$  contained in the representation). We can assume without loss of generality that all bends accounting for the rotation in the center bend in the same direction, thus the edge  $uv$  has  $|\text{rot}(uv[u])| + |\text{rot}(uv[-])| + |\text{rot}(uv[v])|$  bends. Hence, the number of bends depend only on the Kandinsky representation and not on the actual embedding.

Let  $f$  be a face of  $G$  and let  $u$  and  $v$  be two vertices on the boundary of  $f$ . By  $\pi_f(u, v)$  we denote the path from  $u$  to  $v$  on the boundary of  $f$  in clockwise direction (counter-clockwise for the outer face). The rotation  $\text{rot}_f(\pi)$  of a path  $\pi$  in the face  $f$  is defined as the sum of all rotations of edges and inner vertices of  $\pi$  in  $f$ .

Note that an orthogonal embedding (of a graph with maximum degree 4) is basically a Kandinsky embedding without  $0^\circ$  angles at vertices. Thus, we can define *orthogonal representations*, representing an equivalence class of orthogonal embeddings, as Kandinsky representations where rotation 2 at vertices is not allowed (the resulting notion, although it differs slightly, is equivalent to the one introduced by Tamassia [19]).

## 2.3 Network Flows

We will need the following result on the existence of feasible flows in flow networks where the capacity of edges is large compared to the absolute demands of the nodes in network.

**Lemma 1.** *Let  $N = (V, A)$  be a flow network with demands  $d: V \rightarrow \mathbb{R}$  (with  $\sum_{v \in V} d(v) = 0$ ) and capacities  $c: A \rightarrow \mathbb{R}$  such that  $c(e) \geq \sum_{v \in V} |d(v)|$  for all  $e \in E$ . Then there exists a feasible flow in  $N$ .*

*Proof.* Let  $\Phi$  be an arbitrary flow satisfying the demands at all vertices, but possibly violating the capacity constraints. Let  $a = (u, v) \in A$  with  $\Phi(a) > c(e)$ . If there exists a directed path from  $v$  to  $u$  all whose arcs have positive flow, we can decrease the amount of flow on this cycle by 1. After finitely many such steps, we then obtain the desired flow. Hence, assume for the sake of contradiction that such a path does not exist. Let  $S \subseteq V$  be the vertices that can be reached from  $v$ . Note that  $v \in S$  and  $u \notin S$ . Hence,  $S$  defines a cut in  $N$  whose outgoing arcs have flow 0. In any valid flow the amount of flow entering  $S$  minus the flow leaving  $S$  must equal  $\sum_{v \in S} d(v) \leq \sum_{v \in S} |d(v)| \leq \sum_{v \in V} |d(v)| \leq c(e)$ . On the other hand, the flow entering  $S$  is at least  $\Phi(a) > c(e)$  while no flow is leaving  $S$ , a contradiction.  $\square$

## 3 Complexity

Let  $\mathcal{S} = (\mathcal{X}, \mathcal{C})$  be an instance of 3-SAT with variables  $\mathcal{X} = \{x_1, \dots, x_n\}$  and clauses  $\mathcal{C} = \{c_1, \dots, c_m\}$ . A clause is a *positive clause* if it contains only positive literals, a *negative clause* if it contains only negative literals, and a *mixed clause* otherwise. In the *variable-clause graph*, every variable and every clause is a vertex and there is an edge  $xc$  connecting a variable  $x \in \mathcal{X}$  with a clause  $c \in \mathcal{C}$  if and only if  $x \in c$  or  $\neg x \in c$ .

In a *monotone rectilinear representation* of the variable-clause graph, the variables are represented as horizontal line segments on the  $x$ -axis, the positive and negative clauses are represented as horizontal line segments below and above the  $x$ -axis, respectively, and a variable is connected to an adjacent clause by a vertical line segment such that no two line segments cross. Note that an instance admitting a monotone rectilinear representation cannot contain mixed clauses. An instance of PLANAR MONOTONE 3-SAT is an instance  $\mathcal{S} = (\mathcal{X}, \mathcal{C})$  of 3-SAT together with a monotone rectilinear representation of its variable-clause graph; see Figure 3 for an example. De Berg and Khosravi [7] show that PLANAR MONOTONE 3-SAT is NP-hard.

The problem ORTHOGONAL 01-EMBEDDABILITY is defined as follows. Given a 4-plane graph  $G = (V, E)$  and with partitioned edge set  $E = E_0 \cup E_1$ , test whether  $G$  admits an orthogonal drawing such that every edge in  $E_i$  has exactly  $i$  bends. We also refer to the edges in  $E_0$  and  $E_1$  as 0- and 1-edges, respectively. In the following, we always consider the variant of ORTHOGONAL 01-EMBEDDABILITY where we allow to *fix angles at vertices*, that is the value of

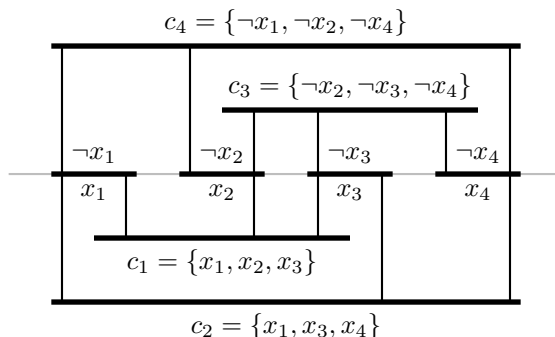


Figure 3: The instance of PLANAR MONOTONE 3-SAT with variables  $x_1, \dots, x_4$  and clauses  $\{x_1, x_2, x_3\}$ ,  $\{x_1, x_3, x_4\}$ ,  $\{\neg x_2, \neg x_3, \neg x_4\}$ , and  $\{\neg x_1, \neg x_2, \neg x_4\}$ .

$\text{rot}_f(v)$  for a vertex  $v$  with incident face  $f$  might be given with the input. Fixing the angles at vertices does not make the problem harder since augmenting a vertex  $v$  to have degree 4 by adding degree-1 vertices incident to  $v$  has the same effect as fixing the angles at  $v$  (when choosing the combinatorial embedding appropriately). Note that this reduces the case with fixed angles at vertices to the one without fixed angles. In the following we implicitly allow angles at vertices to be fixed.

In this section we first show that ORTHOGONAL 01-EMBEDDABILITY is NP-hard by a reduction from PLANAR MONOTONE 3-SAT. Afterwards, we show that KANDINSKY BEND MINIMIZATION is NP-hard by a reduction from ORTHOGONAL 01-EMBEDDABILITY.

### 3.1 Orthogonal 01-Embeddability

Consider a single 1-edge  $e$ . When drawing it, we have to make the decision to either bend it in one or the other direction. In the reduction from PLANAR MONOTONE 3-SAT, this basic decision will encode the decision to set a variable either to **true** or to **false**. In addition to that, the construction consists of several building blocks. For every variable, we need a gadget that outputs its positive and its negative literal. Moreover, we build gadgets representing clauses that admit a correct drawing if and only if at least one out of three edges that require one bend is bent in the desired direction. Since the same literal usually occurs in several clauses, we need to copy the decision made for one edge to several edges. Finally, we need to bring the decisions of the variables to the clauses without restricting the possible drawings of the clauses too much.

In the following we first present some simple gadgets that are used as building blocks in the following constructions. Then we start with the variable gadget that outputs the positive and negative literal of a variable. Afterwards, we show how to duplicate literals and then present the so called bendable pipes that are used to bring the value of a literal to the clauses. Finally, we present the clause gadget. In the end, we put these building blocks together and show

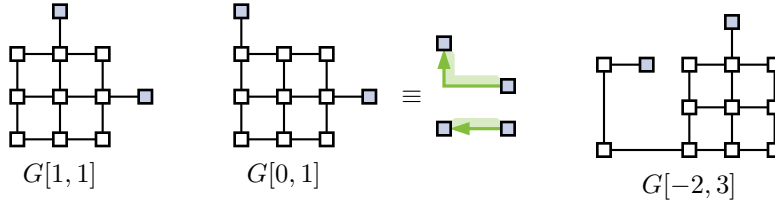


Figure 4: Three different interval gadgets. The vertices  $s$  and  $t$  are marked blue.

the correctness of the construction.

### 3.1.1 Building Blocks

An interval gadget is a small graph  $G[\rho_1, \rho_2]$  with two designated degree-1 vertices (its *endpoints*)  $s$  and  $t$  on the outer face. It has the property that the rotation of  $\pi(s, t)$  is in the interval  $[\rho_1, \rho_2]$  for any orthogonal embedding. The construction is similar to the tendrils used by Garg and Tamassia [14]; see Figure 4 for some examples.

**Lemma 2.** *The interval gadget  $G[\rho_1, \rho_2]$  admits an orthogonal 0-bend drawing with rotation  $\rho$  if and only if  $\rho \in [\rho_1, \rho_2]$ .*

The interval gadget we use most frequently in the following is  $G[0, 1]$ , which behaves like an edge that may have one bend, but only into a fixed direction (recall that the combinatorial embedding of our graph is fixed). To simplify the illustrations, we draw  $G[0, 1]$  as shown in Figure 4 and we refer to them as 01-edges.

To simplify the description of the hardness proof, we next describe a number of basic building blocks, which we combine in different ways to obtain the gadgets for our construction. The building blocks are shown in Figure 5.

Except for the last of the building blocks, each of them consists of a 4-cycle  $s, t, s', t'$ . They only differ in the types of edges. In the *box*  $st$  and  $s't'$  are 1-edges and the other edges are 0-edges; see Figure 5a. In a *bendable box* the two zero-bend edges of a box are replaced by 01-edges directed from  $t$  to  $s'$  and from  $t'$  to  $s$ , respectively; see Figure 5b. In a *merger* the edge  $st$  is a 1-edge,  $s't'$  and  $st'$  are 01-edges (with this orientation) and  $ts'$  is a 0-edge; see Figure 5c. Finally, a *splitter* is a 3-cycle  $s, t, s'$ , where  $ss'$  is a 1-edge and  $s't$  and  $ts$  are 01-edges (with this orientation); see Figure 5d.

Symmetric versions of the bendable box and the splitter can be obtained by reversing the directions of both 01-edges, as shown in Figure 5b,c. Since they differ from the original only by exchanging the inner and outer face and mirroring the instance, their behavior is completely symmetric. Note that, apart from the 0-edges, all edges of the building blocks admit precisely two possible rotation values in each face. Thus, each edge attains its maximum rotation value in one of its incident faces and the minimum rotation in the other one. We call an orthogonal 01-representation of a building block *right-angled* if all

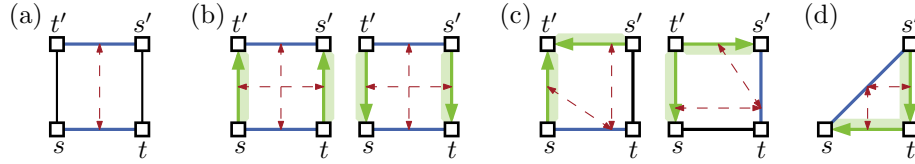


Figure 5: Building blocks for gadgets. The edges are color-coded; 0-edges are black, 1-edges are blue and 01-edges are green and directed such that they may bend right but not left. The building blocks are (a) the box; (b) the bendable box; (c) the merger; (d) the splitter.

inner angles at vertices are  $90^\circ$ . The following lemma states the functionality of these building blocks, which is essentially that in a right-angled orthogonal 01-representation the rotation values of some of the edges are not independent of one another but are linked in the sense that exactly one of them must attain its minimum (maximum) rotation value in  $f$ . In Figure 5 such dependencies are displayed as red dashed arrows. We will later interpret the rotation values as an encoding of truth values. The red dashed arrows then correspond to a transmission of the encoded information.

**Lemma 3.** *Consider a building block  $B$  and assume that we are given rotation values for each of the edges incident to the inner face  $f$  of  $B$  that respect the bend constraints of the edges. The following conditions for each of the building blocks are necessary and sufficient for the existence of a right-angled orthogonal 01-representation of  $B$  respecting the given rotation values.*

1. *Box: Exactly one of  $\{st, s't'\}$  attains its minimum (maximum) rotation in  $f$ .*
2. *Bendable box: Exactly one of  $\{st, s't'\}$  and exactly one of  $\{st', ts'\}$  attains its minimum (maximum) rotation in  $f$ .*
3. *Merger:  $st$  attains its minimum (maximum) rotation in  $f$  if and only if  $st'$  and  $s't'$  attain their maximum (minimum) rotation in  $f$ .*
4. *Splitter:  $st$  attains its minimum (maximum) rotation in  $f$  if and only if  $s't$  and  $t's$  attain their maximum (minimum) rotation in  $f$ .*

*Proof.* We first treat the building blocks that consist of a 4-cycle. Denote the rotation values of  $ts, st', t's'$  and  $s't$  by  $\rho_1, \rho_2, \rho_3, \rho_4$ , respectively. Note that, in any valid drawing, each of the vertices contributes a rotation of 1 to the inner face  $f$ . Since the total rotation around  $f$  must be 4, this implies  $\rho_1 + \rho_2 + \rho_3 + \rho_4 = 0$  is necessary and sufficient for the existence of a valid drawing.

For the box, we have  $\rho_2 = \rho_4 = 0$ , and thus  $\rho_1 = -\rho_3$  is necessary and sufficient, which implies the claim.

For the bendable box, observe that  $\rho_2 \in \{0, 1\}$  and  $\rho_4 \in \{-1, 0\}$ , and thus  $\rho_2 + \rho_4 \in \{-1, 0, 1\}$ . Similarly,  $\rho_1, \rho_3 \in \{-1, 1\}$ , and thus  $\rho_1 + \rho_3 \in \{-2, 0, 2\}$ . To achieve a total sum of 0, it follows that  $\rho_1 + \rho_3 = 0$  and  $\rho_2 + \rho_4 = 0$  is necessary and sufficient. The claim follows.

For the merger observe that  $\rho_4 = 0$ . Moreover, we have  $\rho_2 \in \{0, 1\}$  and  $\rho_3 \in$

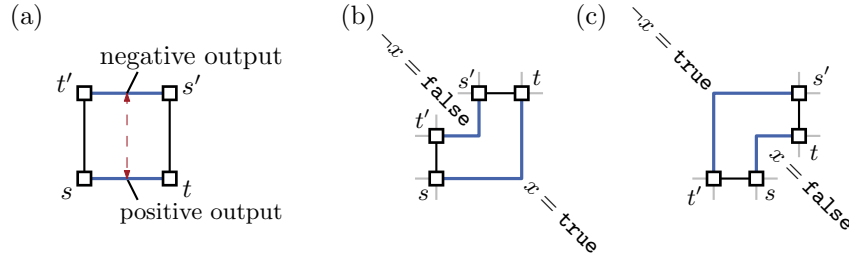


Figure 6: (a) The variable gadget. (b–c) The two possible orthogonal representations corresponding to  $x = \text{true}$  and  $x = \text{false}$ , respectively.

$\{-1, 0\}$ , and thus  $\rho_2 + \rho_3 \in \{-1, 0, 1\}$ . Since  $\rho_1 \in \{-1, 1\}$ , it follows that  $\rho_2 + \rho_3 = 0$  can be excluded. This together with the fact that  $\rho_1 = -\rho_2 - \rho_3$  is necessary and sufficient proves the claim.

Finally, we consider the splitter. We denote the rotations of  $ss'$ ,  $s't$  and  $ts$  in  $f$  by  $\rho_1, \rho_2$  and  $\rho_3$ , respectively. Since each of the three vertices incident to  $f$  supplies a rotation of 1, the existence of a valid drawing is equivalent to  $\rho_1 + \rho_2 + \rho_3 = 1$ . Note that  $\rho_1 \in \{-1, 1\}$ , whereas  $\rho_2, \rho_3 \in \{0, 1\}$ , and thus  $\rho_2 + \rho_3 \in \{0, 1, 2\}$ . It follows immediately that  $\rho_2 + \rho_3 = 1$  is not possible, and thus  $\rho_2 = \rho_3$  is necessary. Then  $\rho_1 = 1 - 2\rho_2$  follows, showing the claim.  $\square$

We will now construct our gadgets from these building blocks. To this end, we take copies of building blocks and glue them together by identifying certain edges (together with their endpoints). As mentioned above, we will use rotations of the 1-edges to encode certain information. Thus, our gadgets will always have such edges on the boundary of the outer face. In the figures, we will again indicate the necessary conditions from Lemma 3 by red dashed edges as in Figure 5. It follows from Lemma 3 that when there is a path of such red edges from one edge to another edge, then they are synchronized. In particular, if both are incident to the outer face than exactly one of them attains the minimum and one of them attains the maximum rotation there in any valid drawing.

### 3.1.2 Gadget Constructions

**Variable Gadget** The variable gadget for a variable  $x$  consists of a single box with vertices  $s, t, s', t'$ . The two 1-bend edges  $st$  and  $s't'$  are called the *positive* and *negative output*, respectively. It immediately follows from Lemma 3 that it has exactly two different valid drawings. We use the interpretation that  $x$  has value **true** if the rotation of the the positive output in the outer face is maximum, and false otherwise; see Figure 6. The following lemma summarizes the properties; it follows immediately from Lemma 3.

**Lemma 4.** *Assume the rotations  $\rho_p$  and  $\rho_n$  of the positive and negative output edges in the outer face are fixed. There is a right-angled orthogonal 01-representations of the variable gadget respecting  $\rho_p$  and  $\rho_n$  if and only if  $\rho_p = -\rho_n \in \{-1, 1\}$ .*

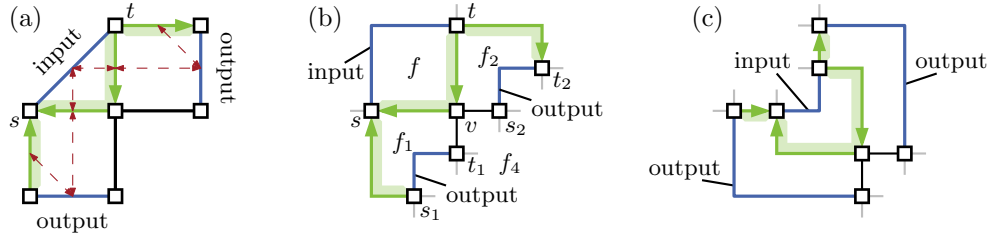


Figure 7: (a) The literal duplicator. (b–c) The two possible orthogonal representations corresponding to the values `false` and `true`, respectively.

**Literal Duplicator** A duplicator is a structure that has three 1-bend edges on the outer face, one of which is the *input edge*, the other two are the *output edges*. The key property is that the structure is such that the state of the inputs is transferred to both outputs in any right-angled orthogonal 01-representation, i.e., the input attains its maximum (minimum) rotation in the outer face if and only if the outputs attain their minimum (maximum) rotation in the outer face. The duplicator is formed by a splitter, which is glued to two mergers via its  $\{0, 1\}$ -edges; see Figure 7. The fact that indeed the information encoded in the input edge is copied to the output edges follows from the red dashed paths connecting the input to the outputs and Lemma 3.

**Lemma 5.** *Assume the rotations  $\rho_i$  of the input edge and the rotations  $\rho_o$  and  $\rho'_o$  of the two output edges in the outer face are fixed. There is a right-angled orthogonal 01-representation of the variable gadget respecting these rotations if and only if  $\rho_i = -\rho_o = -\rho'_o \in \{-1, 1\}$ .*

By concatenating several duplicators in a tree-like fashion, we can of course take as many copies of the state of a literal as there are clauses containing that literal. We make this more precise later.

**Bendable Pipes** The bendable pipe gadget is used for transmitting the information about a literal to a clause. It has an input and an output edge, and has the property that in any valid drawing the information encoded in the input is transmitted to the output. To remedy the fact that the duplicators change their shape depending on the state of the literal they copy, we allow some flexibility of the pipes, allowing them to change how strongly the pipe is bent. This is achieved as follows.

A *zig-zag* consists of a bendable box and a bendable box where the 01-edges are reversed, such that two of their 1-edges are identified. One of the 1-bend edges on the outer face is the input, the other is the output; see Figure 8. It follows immediately from Lemma 3 that the information from the input is transferred to the output. Moreover, it also follows from Lemma 3 that the decision which of the bendable boxes bend their 01-edges can be taken independently. Thus, the zig-zag allows to choose the rotation  $\rho, \rho'$  of the paths between the input and the output edge with  $\rho = -\rho'$  for each  $\rho \in \{-1, 0, 1\}$ .

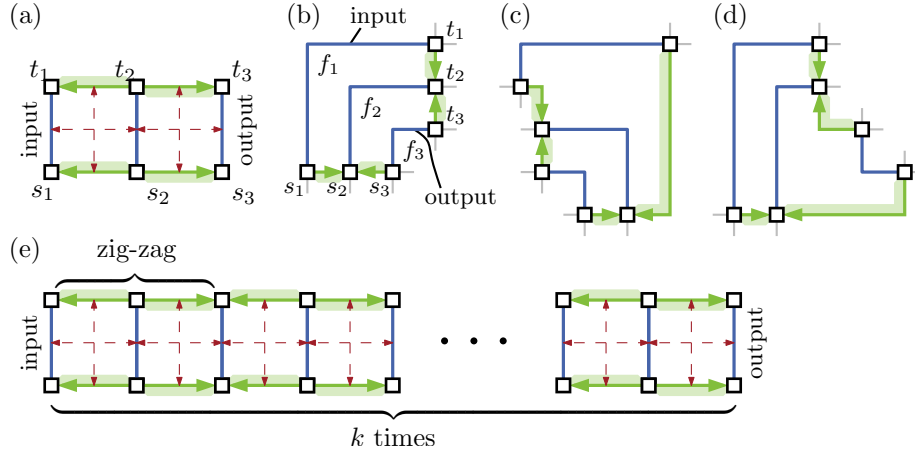


Figure 8: (a) The zig-zag. (b–d) Embeddings of the zig-zag with different rotations 0, 1, and  $-1$  when the input edge has rotation  $-1$  in the outer face. Corresponding drawings where the rotation of the input edge is  $+1$  are symmetric. (e) The  $k$ -bendable pipe.

A  $k$ -bendable pipe is obtained by concatenating  $k$  zig-zags; see Figure 8e. Again Lemma 3 easily implies that the information is transmitted from the input to the output, and moreover, by concatenating suitable drawings of the zig-zags, for each rotation  $\rho \in \{-k, \dots, k\}$ , the paths between the input and the output edge along the outer face can have rotation  $\rho$  and  $-\rho$ , respectively. In a high-level view, a  $k$ -bendable pipe looks like an edge that transfers information between its endpoints and can be bent up to  $k$  times either to the left or to the right. The following lemma summarizes the properties of  $k$ -bendable pipes.

**Lemma 6.** *Assume the rotations  $\rho_i$  and  $\rho_o$  of the input edge and the output edge as well as the rotations  $\rho$  and  $\rho'$  of the two counterclockwise paths on the outer face connecting the input and the output edge are fixed.*

*There is a right-angled orthogonal 01-representations of the  $k$ -bendable pipe if and only if  $\rho_i = -\rho_o \in \{-1, 1\}$  and  $\rho = -\rho' \in \{-k, \dots, k\}$ .*

**Clause Gadget** The clause gadget is a cycle  $C$  of length 4, consisting of three 1-edges, the input edges, and the interval gadget  $G[-2, 3]$ ; see Figure 9a. The embedding is fixed such that the inner face of the clause lies to the right of the interval gadget  $G[-2, 3]$  (that is the rotation of  $G[-2, 3]$  in the inner face lies in the interval  $[-2, 3]$ ). Again we only consider right-angled drawings, where the rotations at the vertices in the internal face are all fixed to 1.

The clause gadget interprets a rotation of  $-1$  for an input edge in the inner face as **true** and a rotation of 1 as **false**. In Figure 9a all three input edges are set to **true**. In Figure 9b two of the three input edges represent the value **false**. In Figure 9c all input edges are **false**, thus  $G[-2, 3]$  would need to have a rotation of  $-3$  in the inner face, which is not possible. The following lemma

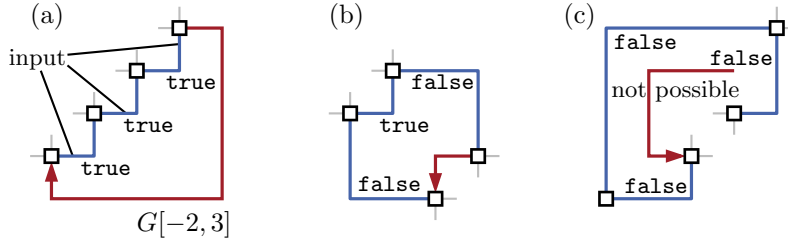


Figure 9: (a–c) The clause gadget with three different values on the input edges.

states more precisely that the clause gadget admits a valid drawing with the given rotations of the input edges if and only if at least one of the input edges represents the value `true`.

**Lemma 7.** *Assume that the rotation  $\rho_1, \rho_2, \rho_3$  of the input edges in the inner face are fixed. There exists a right-angled orthogonal 01-representation of the clause gadget respecting these rotations if and only if  $\rho_i \in \{-1, 1\}$  for  $i \in \{1, 2, 3\}$  and  $\rho_i = -1$  for at least one  $i \in \{1, 2, 3\}$ .*

*Proof.* Each of the four vertices of the clause gadget  $C$  has rotation 1 in the inner face of  $C$ . Thus the sum of the rotations  $\rho_1, \rho_2, \rho_3$ , and the rotation of  $G[-2, 3]$  in the inner face of  $C$  must be 0. The possible rotation of  $G[-2, 3]$  are exactly the integers in the interval  $[-2, 3]$  (Lemma 2). Thus, we get an orthogonal 01-representation if and only if  $\rho_1 + \rho_2 + \rho_3 \in [-3, 2]$ , which is the case if and only if not all three rotations are 1.  $\square$

### 3.1.3 Putting Things Together

Let  $S = (\mathcal{X}, \mathcal{C})$  together with a monotone rectilinear representation be an instance of PLANAR MONOTONE 3-SAT. The plan is to create a variable gadget for every variable and a clause gadget for every clause, duplicate the literals (using the literal duplicator) outputted by the variable gadget as many times as they occur in clauses, and bring the values of the duplicated literals to the input of the clauses using bendable pipes.

Thus, if we have two gadgets  $A$  and  $B$ , we want to use an output edge of  $A$  as the input edge of  $B$ . To make the description simpler, we assume each input edge and each output edge of the gadgets to be oriented such that the outer face lies to its left and to its right, respectively. We can combine  $A$  and  $B$  by identifying an output edge  $e_A$  of  $A$  with an input edge  $e_B$  of  $B$  such that their sources and targets coincide. All input and output edges of the two gadgets remain input and output edges in the resulting graph, except for  $e_A$  and  $e_B$ .

Let  $x \in \mathcal{X}$  be a variable. We take one variable gadget  $X$  representing the decision made for  $x$ . Let  $k$  be the number of clauses containing the literal  $x$ . We successively add  $k - 1$  literal duplicators. The input edge of the first literal duplicator is identified with the positive output edge of  $X$ . The input edge of every following literal duplicator is identified with an output edge of a previously

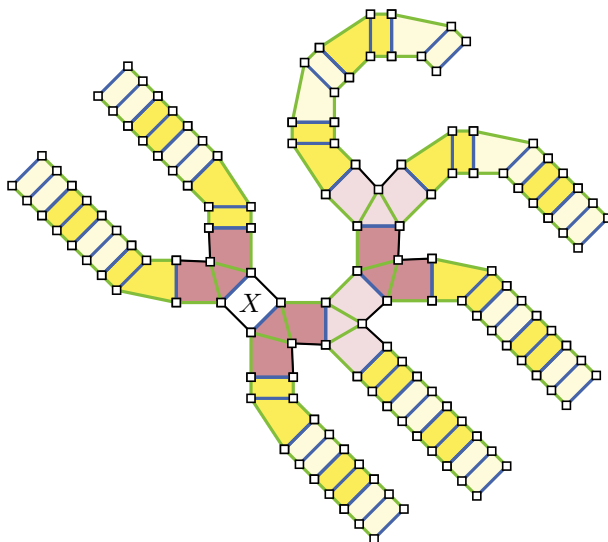


Figure 10: Variable tree  $T_x$  of a variable  $x$  whose positive and negative literal have five and two occurrences, respectively. The variable gadget is shaded white, duplicators are shaded in red and zig-zags (forming bendable pipes) are shaded yellow. Adjacent gadgets of the same type are shaded with different saturations.

added literal duplicator. The graph we get has the negative output edge at  $X$  and  $k$  output edges belonging to literal duplicators. To each of these  $k$  output edges we add a  $K$ -bendable pipe for a suitably large  $K$  by identifying the output edge with the input edge of the bendable pipe. We choose  $K = 3m^2 + 4m$ , where  $m$  is the number of edges in the variable-clause graph of  $S$ . Let  $k'$  be the number of clauses containing the literal  $\neg x$ . As for the positive literal, we add  $k' - 1$  literal duplicators, this time identifying the input edge of the first literal duplicator with the negative output edge of  $X$ . As before, we also add  $K$ -bendable pipes to each of the  $k'$  output edges. We call the resulting graph *variable tree of  $x$*  and denote it by  $T_x$ . We call the  $k$  output edges of the bendable pipes attached to literal duplicators attached to the positive output edge of the variable gadget  $X$  the *positive output edges* of  $T_x$ . The  $k'$  other output edges are *negative output edges* of  $T_x$ . The variable tree for the case  $k = 5$  and  $k' = 2$  is illustrated in Figure 10.

For the instance  $S = (\mathcal{X}, \mathcal{C})$  of PLANAR MONOTONE 3-SAT we create the following instance of ORTHOGONAL 01-EMBEDDABILITY. For every variable  $x \in \mathcal{X}$ , we take the variable tree  $T_x$ . For every clause  $c \in \mathcal{C}$ , we add a copy of the clause gadget. We connect them by identifying the output edges of the variable trees with the input edges of the clause gadget in the following way.

Consider a variable  $x$  and a positive clause  $c$  with  $x \in c$  in the monotone rectilinear representation of  $S$ . We say that  $c$  is the  *$i$ th positive clause* of  $x$  if the edge connecting  $c$  and  $x$  is the  $i$ th edge incident to  $x$  (ordered from left to

right). Analogously,  $x$  is the  $j$ th variable of  $c$  if this edge is the  $j$ th edge incident to  $c$ . In the instance shown in Figure 3 and Figure 11, the clause  $c_1$  is the first positive clause of  $x_2$  and  $x_2$  is the second variable of  $c_1$ . Analogously, we define the  $i$ th negative clause.

Let  $c$  be the  $i$ th positive clause of  $x$  and let  $x$  be the  $j$ th variable of  $c$ . Let further  $C$  be the clause gadget corresponding to  $c$ . Traversing the outer face of  $C$  in counter-clockwise order starting with the interval gadget defines an order on the input edges of  $C$ . Moreover, traversing the variable tree  $T_x$  in counter-clockwise order starting with an edge incident to the variable gadget defines an order on the positive output edges of  $T_x$ . We identify the  $i$ th positive output edge of  $T_x$  with the  $j$ th input edge of  $C$ . For a negative clause containing  $\neg x$ , we do exactly the same except for defining the order of the negative output edges by traversing the outer face of  $T_x$  in clockwise order. This identification of input with output edges is done for every edge in the variable-clause graph. We denote the resulting graph by  $G(S)$ . Figure 11 shows the monotone rectilinear representation (rotated by  $45^\circ$ ) of an example instance  $S$  and the graph  $G(S)$ . The graph  $G(S)$  has two kinds of faces. Faces that are inner faces in the variable tree or in the clause gadget are called *small faces*. The other faces are *large faces*. Note that there is a one-to-one correspondence between the large faces of  $G(S)$  and the faces of the variable-clause graph of  $S$ . We obtain the following theorem by proving that  $S$  admits a satisfying truth assignment if and only if  $G(S)$  admits an orthogonal 01-representation.

**Theorem 1.** ORTHOGONAL 01-EMBEDDABILITY *is NP-complete.*

*Proof.* Let  $S = (\mathcal{X}, \mathcal{C})$  be an instance of MONOTONE PLANAR 3-SAT and let  $G(S)$  be the graph constructed from  $S$  as defined above. We first show that the existence of an orthogonal 01-representation of  $G(S)$  implies the existence of a satisfying truth assignment for  $S$ .

Let  $\mathcal{O}$  be an orthogonal 01-representation of  $G(S)$ . Let  $x \in \mathcal{X}$  be a variable and let  $X$  be the corresponding variable gadget in  $G(S)$ . If the positive output edge of  $X$  has rotation  $-1$  in its outer face, we set  $x = \mathbf{true}$  (as illustrated in Figure 6b). Otherwise, we set  $x = \mathbf{false}$  (as illustrated in Figure 6c). We claim that this gives a satisfying truth assignment for  $S$ . Let  $c \in \mathcal{C}$  be a positive clause and let  $C$  be the corresponding clause gadget in  $G(S)$ . By Lemma 7, at least one of the input edges of  $C$  has rotation  $-1$  in its inner face. By construction of  $G(S)$ , this input edge is identified with an positive output edge of the variable tree  $T_x$  for a variable  $x$ . Let  $X$  be the corresponding variable gadget. As there is a path of literal duplicators and bendable pipes from the positive output edge of  $X$  to every positive output edge of  $T_x$ , it follows from Lemma 5 and Lemma 6 that the positive output edge of  $X$  has rotation  $-1$  in its outer face if and only if any positive output edge of  $T_x$  has rotation  $-1$  in the outer face of  $T_x$ . Thus, it follows that the positive output edge of  $X$  has rotation  $-1$  in its outer face and thus  $x = \mathbf{true}$ , which satisfies the clause  $c$ .

If  $c$  is a negative clause, we find a variable  $x$  such that the negative output edge of the corresponding variable gadget  $X$  has rotation  $-1$  in its outer face.

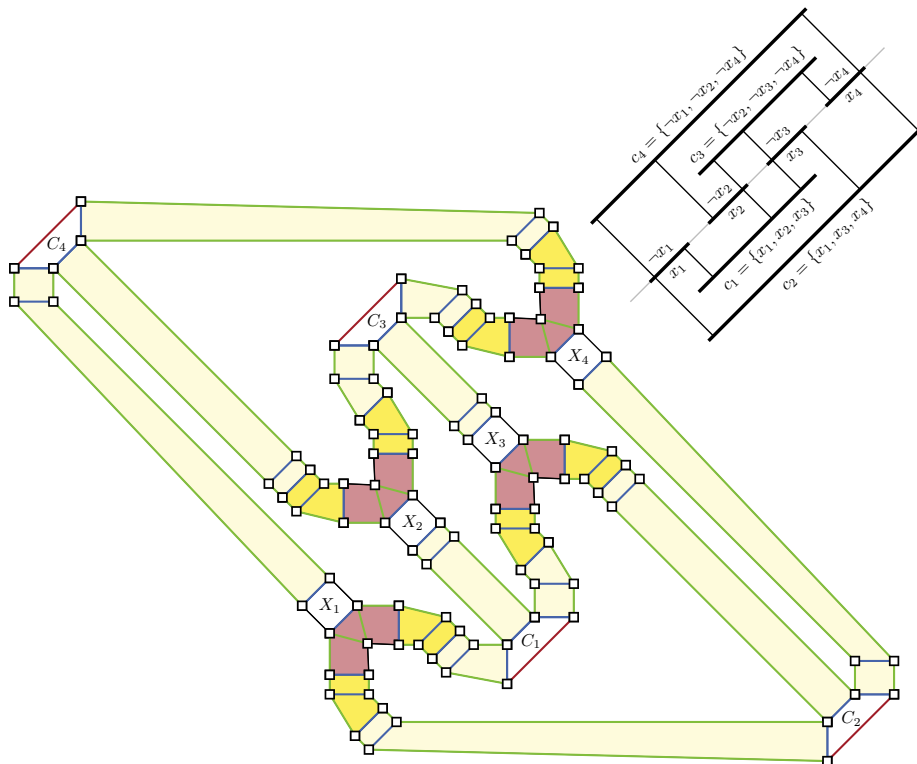


Figure 11: Example reduction of PLANAR MONOTONE 3-SAT to ORTHOGONAL 01-EMBEDDABILITY. The bendable pipes have been shortened for clarity.

By Lemma 4, the positive output edge of  $X$  has rotation 1 in its outer face, thus  $x = \text{false}$  holds, which satisfies the negative clause  $c$  containing  $\neg x$ .

It remains to show the opposite direction. Assume we have a satisfying truth assignment for  $S$ . We show how to construct an orthogonal 01-representation of  $G(S)$ . As  $G(S)$  consists of gadgets for which the rotations around every vertex are fixed, it remains to specify a rotation for every edge such that the rotation around every inner face is 4. We start with the small faces. Consider the variable tree  $T_x$  of a variable  $x$  containing the variable gadget  $X$ . If  $x = \text{true}$ , we choose the orthogonal 01-representation of  $X$  where the positive output edge has rotation  $-1$ . This yields a feasible representation by Lemma 4; see Figure 6b–c.

This already fixes the rotation of the literal duplicators in  $T_x$  that are directly attached to the output edges of  $X$ . By Lemma 5 this fixes the rotation of the corresponding output edge (to the same behavior as the input edge) and a corresponding orthogonal 01-representation of the duplicator exists; see Figure 7b–c. Applying this procedure iteratively to every literal duplicator whose input edge has a fixed rotation fixes the orthogonal representation of every literal duplicator in  $T_x$ .

Similarly, we (partially) fix the orthogonal 01-representation of the bendable pipes contained in  $T_x$  iteratively according to Lemma 6. More precisely, the rotation of the 1-edges is fixed according to the rotation of the input edge; see Figure 8e. However, we do not fix the rotation of the bendable pipes. Recall that, by Lemma 6 this rotation can be anything in  $\{-K, \dots, K\}$ . We will need the flexibility of choosing this rotation to get the rotations in the large faces right.

Note that the resulting orthogonal 01-representations of the variable tree have the following properties. The positive output edges of  $T_x$  have rotation  $-1$  if  $x = \text{true}$  and rotation  $1$  otherwise. The negative output edges have rotation  $-1$  if  $\neg x = \text{true}$  and rotation  $1$  otherwise. By fixing the orthogonal representations of the variable trees in this way, we already fix the orthogonal representation of the input edges of the clause gadgets in  $G(S)$ . Let  $C$  be a clause gadget in  $G(S)$ . Since  $S$  is a satisfying truth assignment, it follows that the rotation of at least one input edge of  $C$  in the inner face of  $C$  is  $-1$ . Thus,  $C$  admits an orthogonal 01-representation by Lemma 7. The choices made so far imply that every small face in our orthogonal 01-representation has rotation 4, as required.

It remains to choose the rotations of the bendable pipes such that the rotation in the large inner faces is 4. Initially, assume that the rotation of every bendable pipe is 0. We first bound the maximum deviation from a rotation of 4 around large faces.

Let  $f$  be a large face and let  $f_S$  be the corresponding face in the variable-clause graph of  $S$ . The boundary of  $f$  can be naturally subdivided into paths belonging to different variable trees and paths on the outer face of clause gadgets. Let  $x$  be a variable on the boundary of  $f_S$ . A path between two output edges of  $T_x$  consists of three subpaths. Two paths with rotation 0 consisting of edges belonging to bendable pipes and, in between, one path of edges belonging to literal duplicators. Clearly, this path has length at most  $\deg(x)$  and since the absolute value of the rotation at edges and vertices is at most 1, we get a total rotation between  $-2\deg(x)$  and  $2\deg(x)$  in the large face. Summing over all variables incident to  $f_S$  gives us a rotation between  $-2m$  and  $2m$ , where  $m$  is the number of edges in the variable-clause graph. Moreover, for each clause incident to  $f_S$  the boundary of  $f$  contains a path having absolute rotation at most 3. As there are  $m/3$  clauses, the total rotation around the large face  $f$  is between  $-3m$  and  $3m$ .

Changing the rotation of a bendable pipe increases the rotation of one incident large face by 1 and decreases it in the other incident large face by  $-1$ . (Note that this does not affect the rotations at small faces.) Thus, choosing the rotations of the bendable pipes such that the rotation in every large face is 4 (except for the outer face with rotation  $-4$ ) is equivalent to finding a flow in the flow network  $N$  defined as follows. The underlying graph of  $N$  is the dual graph of the variable-clause graph of  $S$ . The demand of the node corresponding to the face  $f_S$  is the difference between the rotation in the corresponding large face  $f$  of  $G(S)$  and 4 ( $-4$  if  $f$  is the outer face). Note that the demands sum up to 0. The capacity on an edge connecting  $f_S$  and  $f'_S$  is equal to the total length

of the bendable pipes incident to the corresponding faces  $f$  and  $f'$  in  $G(S)$ , and thus at least  $K$ . As shown above, the absolute value of the demand of each node in the flow network is at most  $3m + 4$ . As the flow network contains at most  $m$  nodes (otherwise it would be a tree or disconnected), the sum of the absolute values of the demands is bounded by  $3m^2 + 4m$ . The capacity of every edge in  $N$  is at least  $K = 3m^2 + 4m$  by the construction of the variable tree. By Lemma 1 the network  $N$  has a solution.  $\square$

**Theorem 2.** *ORTHOGONAL 01-EMBEDDABILITY is NP-hard for all combinations of the following variations.*

- *The input has a fixed planar embedding or a fixed planar embedding up to the choice of an outer face.*
- *The angles at vertices incident to 1-edges are fixed or variable, while angles at vertices incident to 0-edges are variable.*

*Proof.* In the construction showing Theorem 1, we already fixed all angles at vertices incident to 1-edges (the only vertices whose angles are not fixed lie inside interval gadgets). Thus, we already established hardness for the case that all angles at vertices incident to 1-edges are fixed. As mentioned before, fixing angles is not a really a restriction, as we can enforce fixed angles by attaching degree-1 vertices.

It remains to show that the problem remains hard when allowing to choose a different outer face. Clearly, when choosing a different large face as outer face all arguments leading to a satisfying truth assignment remain valid. Moreover, choosing a small face as outer face can never lead to a valid orthogonal 01-representation for the following reason. Each small face is one of the building blocks presented in Section 3.1.1 (see Figure 5), or the inner face of a clause gadget (Figure 9). For the building blocks it is easy to see that the total rotation in the inner face is at least 0 (by the fixed angles and the restriction of bends on the edges). Thus, none of them can be chosen as the outer face (which would require a rotation of  $-4$ ). Similarly, the rotations at every vertex in the clause gadget is 1 in its inner face, which sums up to a rotation of 4. The three input edges have rotation at least  $-1$  in the inner face and the interval gadget has rotation at least  $-2$ . Thus, the total rotation is at least  $-1$ , which makes it impossible to choose it as the outer face.  $\square$

By the equivalence of orthogonal representations to flow networks [19], it follows that it is NP-hard to test whether there is a valid flow in a planar flow network with the properties that (i) the capacity on every edge is 1 and (ii) some undirected edges require to have one unit of flow (no matter in which direction). Note that Garg and Tamassia [14] show hardness for the less restrictive case that the capacities and the lower bounds for flow on undirected edges is unbounded. They use this to show NP-hardness of ORTHOGONAL 0-EMBEDDABILITY of 4-planar graph (with variable combinatorial embedding).

**Theorem 3.** *All variants of ORTHOGONAL 01-EMBEDDABILITY are NP-hard even if the input graph is a subdivision of a 3-connected graph.*

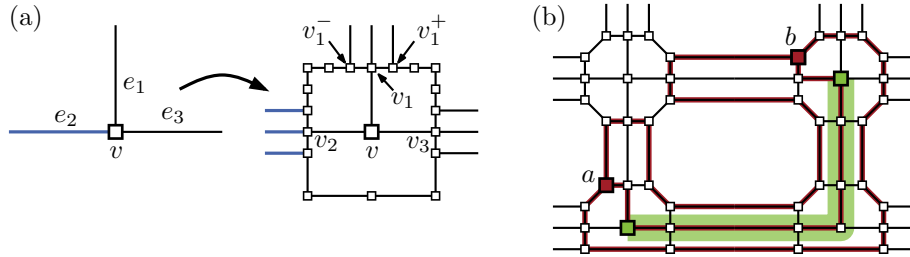


Figure 12: (a) Construction for transforming an instance of ORTHOGONAL 01-EMBEDDABILITY into a subdivision of a 3-connected graph. A vertex  $v$  of degree 3 with variable angles (left) and the corresponding gadget for the construction (rights). (b) The routing of three disjoint paths from  $a$  to  $b$  in  $G'$ ; subdivision vertices are omitted. Vertices  $u$  and  $v$  are marked green, and the corresponding path in  $G$  is bold green. The three red paths between  $a$  and  $b$  follow the bold green path. Note that at the beginning at the end of a path some rerouting via vertices not on the path may be necessary, however, the rerouting is such that the paths remain disjoint.

*Proof.* We reduce from ORTHOGONAL 01-EMBEDDABILITY with fixed planar embedding and variable angles. Let  $G = (V, E_0 \cup E_1)$  be a connected instance of this problem. We replace each degree-1 vertex  $v$  by a cycle  $C$  of four 0-edges such that one vertex of  $C$  is adjacent to the neighbor of  $v$ . It is not hard to see that the resulting graph has an orthogonal 01-embedding if and only if  $G$  has one. In the following we assume without loss of generality that  $G$  has minimum degree 2.

For each vertex  $v$  with incident edges  $e_1, \dots, e_d$  (in clockwise order around  $v$ ), we make the following construction. First, we subdivide its incident edges  $e_i$  with new vertices  $v_i$  and connect them to form a cycle (in the clockwise ordering around  $v$ ), and subdivide the edges of this cycle five times. The vertices before and after  $v_i$  in clockwise direction are denoted  $v_i^-$  and  $v_i^+$ . Afterwards, each edge  $uv$  has been subdivided into  $uu_i, u_i v_j, v_j v$ . We now add for each such edge the edges  $u_i^- v_j^+$  and  $u_i^+ v_j^-$ . The edges  $u_i v_j, u_i^- v_j^+$ , and  $u_i^+ v_j^-$  are 1-edges if and only if the original edge  $uv$  was a 1-edge. All other edges are 0-edges. Figure 12a illustrates the construction for a vertex of degree 3.

We claim that the resulting graph  $G'$  (i) admits an orthogonal 01-representation if and only if  $G$  does, and (ii) is a subdivision of a 3-connected graph. Once the claim is proved, the statement of the theorem follows since the reduction can be performed in polynomial time.

We start with (i). First assume that  $G'$  has an orthogonal 01-representation  $\mathcal{O}$  and let  $uv$  be an edge of  $G$  that is subdivided into  $u_i v_j$ . By construction both  $u_i$  and  $v_j$  have degree 4 and the edges  $uu_i$  and  $v_j v$  are 0-edges. That is all bends of the path  $uu_i v_j v$  lie on the edge  $u_i v_j$ . Hence, the representation on the subgraph containing the vertices  $\{v, v_1, \dots, v_{\deg(v)} \mid v \in V\}$  has all bends on the edges  $v_i v_j$ . We can then undo the subdivisions and obtain an orthogonal 01-

representation of  $G$ . Conversely, if  $\mathcal{O}$  is an orthogonal 01-representation of  $G$ , we can first subdivide each edge  $uv$  close to vertices  $u$  and  $v$  to obtain vertices  $u_i$  and  $v_j$  with  $uu_i$  and  $v_jv$  having 0 bends. Then we add the edges the edges  $u_i^-v_j^+$  and  $u_i^+,v_j^-$  parallel to  $u_iv_j$ . Finally, we add the remaining edges of the cycle around  $v$ , which can be done without bends on the edges since the paths from  $v_i^+$  to  $v_{i+1}^-$  (indices taken modulo  $\deg(v)$ ) have sufficiently many degree-2 vertices, which can serve as bends. We have obtained an orthogonal 01-representation of  $G'$ .

For (ii), we show that in  $G'$  any two vertices  $a$  and  $b$  of degree 3 or more are connected by three (internally) vertex-disjoint paths. Let  $u$  and  $v$  be the two vertices of  $G$  to whose construction  $a$  and  $b$  belong. If  $u = v$  it is not hard to find three disjoint paths; one path goes through the center vertex  $v$ , the remaining paths are routed clockwise and counterclockwise along the cycle around  $v$ . It may be necessary to route through a neighboring gadget to get around the attachment vertices of  $v$ ; see Figure 12b.

If  $u \neq v$ , we pick a shortest path  $u = u_1, \dots, u_k = v$  from  $u$  to  $v$  in  $G$ . This path corresponds to a path  $u_1a_1b_2u_2, \dots, a_{k-1}b_ku_k$ , where  $a_i$  and  $b_i$  are vertices of the cycle around vertex  $u_i$ . We find three disjoint paths from  $a_1^-, a_1$  and  $a_1^+$  to  $b_k^-, b_k$  and  $b_k^+$ , respectively, simply by taking for each edge  $u_iu_{i+1}$  for  $1 < i < k - 1$  the path from  $a_i^+$  in clockwise direction along the cycle around  $u_i$  via  $b_i^-$  to  $a_{i+1}^+$ , from  $a_i$  via the center vertex  $u_i$  and  $b_i$  to  $a_{i+1}$ , and from  $a_i^-$  in counterclockwise direction along the cycle around  $u_i$  via  $b_i^+$  to  $a_{i+1}^-$ ; this is illustrated in the middle vertex of the green path in Figure 12b. We also extend these paths by adding edges  $a_{k-1}b_k, a_{k-1}^+b_k^-$  and  $a_{k-1}^-b_k^+$  so that we have disjoint paths from  $a_1^-$  to  $b_k^+$ , from  $a_1$  to  $b_k$  and from  $a_1^+$  to  $b_k^-$ . It then remains to find disjoint paths from  $a$  to  $a_1^-, a_1$  and  $a_1^+$  and from  $b_k^-, b_k$  and  $b_k^+$  to  $b$ . This can be done by routing in the gadget around  $u$  and  $v$ , respectively. Note that it may be necessary to visit the gadget of an adjacent vertex. This does, however, not interfere with the paths constructed so far since we assumed that it is a shortest path, and hence the corresponding neighbors are not part of the constructed paths. This finishes the proof of the claim.  $\square$

**Corollary 1.** *ORTHOGONAL 0-EMBEDDABILITY is NP-hard for 4-planar graphs with a variable combinatorial embedding.*

*Proof.* We reduce from *ORTHOGONAL 01-EMBEDDABILITY* where the input graph is a subdivision of a 3-connected graph. Note that the embedding is unique up to the choice of the outer face. We now replace each 1-edge by a copy of the interval gadget  $G[1, 1]$  (see Figure 4). Changing the embedding of this gadget decides the bend direction of the 1-edge and vice versa. It is not hard to see that the resulting graph admits a 0-embedding if and only if the original instance admits an orthogonal 01-embedding. Clearly the reduction runs in polynomial time.  $\square$

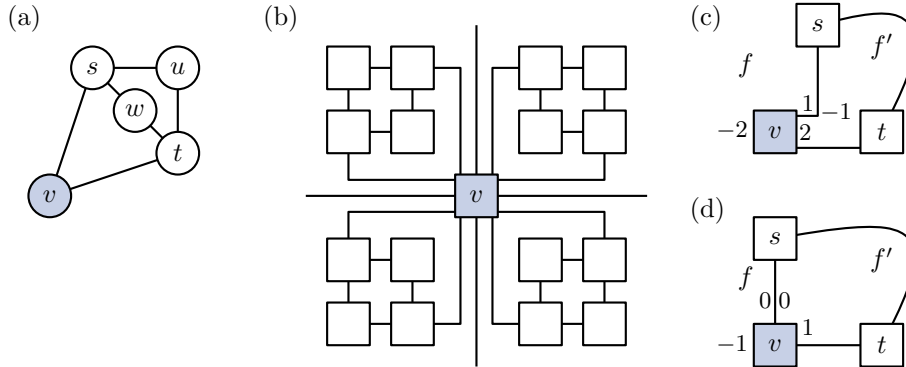


Figure 13: (a) A corner blocker with attachment vertex  $v$ . (b) A Kandinsky representation of a vertex  $v$  with four attached corner blockers (and four outgoing edges). (c-d) Illustration of the proof of Lemma 8.

### 3.2 Kandinsky Bend Minimization

In the following, we show how to reduce ORTHOGONAL 01-EMBEDDABILITY to KANDINSKY BEND MINIMIZATION. The reduction consists of two basic building blocks. In an orthogonal embedding, every side of a vertex can be occupied by at most one edge. We show how to enforce this requirement also for Kandinsky embeddings. Moreover, we construct a subgraph whose Kandinsky embeddings behave like the embeddings of an edge with exactly one bend.

**Corner Blocker** Let  $B$  be the graph consisting of a 4-cycle together with an additional *attachment vertex* connected to two non-adjacent vertices of the 4-cycle. The graph  $B$  is called *corner blocker*. Figure 13a shows a corner blocker with attachment vertex  $v$ . Let  $v$  be a vertex in a planar graph  $G$ . *Blocking a corner of  $v$*  denotes the process of attaching a corner blocker to  $v$  by identifying the attachment vertex of  $B$  with  $v$ . Consider a Kandinsky embedding of  $G + B$ . The corners of the box representing the vertex  $v$  are also called the *corners of  $v$* . We say that a corner of  $v$  is *blocked* by the corner blocker  $B$  if it lies in the inner face of  $B$  incident to  $v$ . Figure 13b shows a vertex  $v$  with four corner blockers attached to it such that all four corners of  $v$  are blocked. Note that the Kandinsky representation of a Kandinsky embedding already determines which corners are blocked by a corner blocker.

The idea behind the corner blocker is to enforce a blocking of all four corners of a vertex. Recall that we assume a fixed planar embedding of the input graph and thus a fixed order of edges around every vertex. Thus, blocking all four corners is equivalent to enforcing edges to leave a vertex at a specific side, as in Figure 13b. The following two lemmas show that the corner blocker defined above is well suited for this purpose, as it admits an optimal drawing blocking only a single corner but blocking no corner causes additional cost.

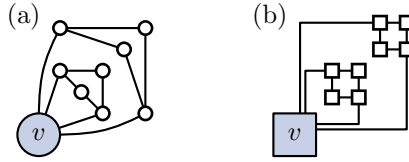


Figure 14: (a) The nested corner blocker  $B_2$  of depth 2. (b) Kandinsky representation of  $B_2$  with 4 bends.

**Lemma 8.** *Every Kandinsky representation of a corner blocker has at least two bends.*

*Proof.* Let  $B$  be a corner blocker. Denote the degree-2 vertices of  $B$  with  $u$ ,  $v$ , and  $w$  and the degree-3 vertices with  $s$  and  $t$  and let  $B$  be embedded such that the boundary of the outer face  $f$  contains  $u$ ,  $v$ ,  $s$ , and  $t$ ; see Figure 13a. In every Kandinsky representation, the total rotation around  $f$  is  $-4$ . We show that this already implies that every Kandinsky representation has at least two bends.

Let  $f'$  be the inner face incident to  $v$ . If  $v$  has rotation 2 in  $f'$  for a fixed Kandinsky representation, then one of the two edges  $vs$  or  $vt$  has rotation  $-1$  at  $v$ . We assume without loss of generality that  $vs$  has rotation  $-1$  at  $v$ , thus we get the following rotation values (see Figure 13c):  $\text{rot}_{f'}(v) = 2$ ,  $\text{rot}_f(v) = -2$ ,  $\text{rot}_{f'}(vs[v]) = -1$ , and  $\text{rot}_f(vs[v]) = 1$ . As  $v$  has degree 2, we obtain another Kandinsky representation by setting  $\text{rot}_{f'}(v) = 1$ ,  $\text{rot}_f(v) = -1$ ,  $\text{rot}_{f'}(vs[v]) = 0$ , and  $\text{rot}_f(vs[v]) = 0$ ; see Figure 13d. As this new Kandinsky representation has fewer bends, we can assume in the following that  $\text{rot}_{f'}(v) \neq 2$ , which shows that the rotation at  $v$  in  $f$  is at least  $-1$ . Clearly, the same holds for  $u$ .

A similar argument shows that the rotations at  $s$  and  $t$  in  $f$  are at least 0. It follows that the total rotation of vertices in the outer face is at least  $-2$ . Thus, to get a total rotation of  $-4$ , there need to be two bends on edges incident to the outer face, which shows the claim.  $\square$

**Lemma 9.** *Every Kandinsky representation of a corner blocker that blocks no corner of its attachment vertex has at least three bends.*

*Proof.* As shown in the proof of Lemma 8, one can reduce the number of bends of a Kandinsky representation of a corner blocker if the rotation at the attachment vertex in the outer face is  $-2$ ; see Figure 13c,d.  $\square$

We can make the corner blockers stronger by nesting them. The *nested corner blocker*  $B_d$  of depth  $d$  is obtained by taking  $d$  corner blockers and identifying their attachment vertices. The nested corner blocker  $B_d$  is embedded such that  $v$  lies on the outer face and the innermost face has distance  $d$  to the outer face (in the dual graph); see Figure 14 for an example. Clearly, the statements from Lemma 8 and Lemma 9 extend to nested corner blockers, where all bend numbers have to be multiplied with  $d$ .

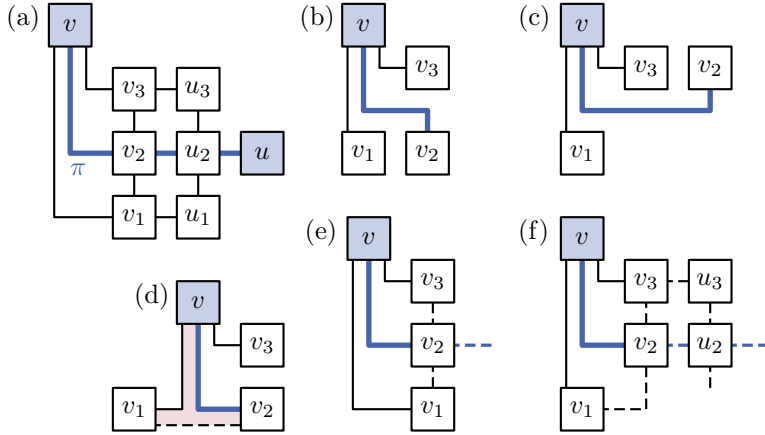


Figure 15: (a) The one bend gadget  $\Gamma$  with three bends without blocked corners at  $v$  with  $|\text{rot}(\pi)| = 1$ . (b–c) The two possible representations of the edges incident to  $v$ , when  $vv_2$  (blue) has two bends. Both cannot be extended to  $\Gamma$  without additional bends. (d–f) The possible ways to draw  $vv_1$ , when  $vv_2$  (blue) has one bend together with the implied drawing on some other edges (dashed). Either we get no Kandinsky representation of  $\Gamma$  (d), or the path  $\pi$  has absolute rotation 1 (e–f).

**One-Bend Gadget** Let  $\Gamma$  be the graph consisting of the  $2 \times 3$ -grid with the two columns  $v_1, v_2, v_3$  and  $u_1, u_2, u_3$  (from bottom to top) together with the vertex  $v$  connected to  $v_1, v_2$ , and  $v_3$  and the vertex  $u$  connected to  $u_2$ ; see Figure 15a. We call  $\Gamma$  the *one-bend gadget* with its two *endvertices*  $u$  and  $v$ . The path  $\pi = (u, u_2, v_2, v)$  is called the *bending path* of  $\Gamma$ . In the following we show that the bending path of a one-bend gadget is (more or less) forced to have either rotation 1 or  $-1$  in every Kandinsky representation. As for the corner blocker, we say that the one-bend gadget blocks  $k$  corners of the vertex  $v$  in a given Kandinsky representation if  $k$  corners of  $v$  lie in the inner face of  $\Gamma$ .

**Lemma 10.** *Let  $\mathcal{K}$  be a bend-minimal Kandinsky representation of the one-bend gadget  $\Gamma$  blocking no corner of its degree-3 endvertex. Then  $\mathcal{K}$  has three bends and the rotation of the bending path in  $\Gamma$  is either 1 or  $-1$ .*

*Proof.* Note that the Kandinsky representation of  $\Gamma$  in Figure 15a does not block a corner of  $v$  and has three bends. It remains to show that this drawing is optimal and that the rotation of the bending path  $\pi$  is always 1 or  $-1$ .

We consider all Kandinsky representations of  $\Gamma$  with at most three bends blocking no corner of  $v$  and show that each of these representations has three bends and rotation 1 or  $-1$  on  $\pi$ . We start with two simple facts. First, blocking no corner of  $v$  requires that at least two of the edges  $vv_1, vv_2$ , and  $vv_3$  to have a bend, as they all leave  $v$  at the same side. Second, the edges in each of the triangles  $vv_1v_2$  and  $vv_2v_3$  require at least two bends, as they have rotation 2 at  $v$ . We use these facts several times in the following case distinction on the

number of bends of  $vv_2$ .

Assume  **$vv_2$  has three bends**. As at least two of the edges  $vv_1$ ,  $vv_2$ , and  $vv_3$  have bends, we get at least four bends in total (but we consider only drawings with at most three bends). Assume that  **$vv_2$  has zero bends**. Then the two bends of the triangle  $vv_1v_2$  must be on the edges  $vv_1$  and  $v_1v_2$  and the bends of the triangle  $vv_2v_3$  must be on the edges  $vv_3$  and  $v_2v_3$ . Thus, there are at least four bends, which again contradicts the restriction to at most three bends.

If  **$vv_2$  has two bends**, one of the two edges  $vv_1$  or  $vv_3$  has one bend, the other has no bend (as we have more than three bends otherwise). Assume that  $vv_3$  has one bend, the other case is symmetric. As  $vv_1$  has no bend, the direction of the bend of  $vv_3$  and of the first bend of  $vv_2$  is fixed. The remaining choice is the second bend of  $vv_2$ ; see Figure 15b and c for an illustration of the two possible Kandinsky representations. Since we already used three bends, the  $2 \times 3$  grid consisting of the nodes  $v_1 \dots v_3$  and  $u_1 \dots u_3$  must be drawn without any bends. However, the Kandinsky representation without bends of the  $2 \times 3$  grid is unique (see Figure 15a) and can obviously not be merged with one of the Kandinsky representations of the three edges incident to  $v$  shown in Figure 15b and c.

Assume that  **$vv_2$  has one bend**. Assume without loss of generality that the bend on  $vv_2$  is a left bend, when traversing it from  $v$  to  $v_2$  (i.e.,  $vv_2$  has rotation 1 in the triangle  $vv_2v_3$ ). This implies that the edge  $vv_3$  has at least one bend as in Figure 15d–f. If  $vv_1$  has a bend but in the other direction then all remaining edges have to be straight, which is not possible for  $v_1v_2$  without creating an empty triangle (Figure 15d). Thus,  $v_1v_2$  has either a bend in the same direction as  $vv_1$  or no bend. Consider the former case first; see Figure 15e. We split the bending path  $\pi$  into two parts, the edge  $vv_2$  and the path from  $v_2$  to  $u$ . Clearly, the absolute rotation of  $vv_2$  is 1. As we already used three bends, the Kandinsky representation of  $\Gamma - v$  is unique. Thus, the path from  $v_2$  to  $u$  must have rotation 0. To show  $|\text{rot}(\pi)| = 1$ , it remains to show that the rotation of  $\pi$  at  $v_2$  is 0, which is the case if there is no  $0^\circ$  angle at  $v_2$ . This angle would have to be adjacent to the edge  $vv_2$  as it is the only one having a bend. However,  $vv_2$  has only one bend and, since  $\text{rot}_f(vv_2[v]) = 1$ , it follows that  $\text{rot}_f(vv_2[v_2]) = 0$ , where  $f$  is the face bounded by  $vv_2v_3$ . But then there can be no  $0^\circ$  bend at  $v_2$ .

It remains to deal with the case that  $vv_1$  has no bend; see Figure 15f. As the triangle  $vv_1v_2$  needs two bends, the edge  $v_1v_2$  must be drawn with a bend. All remaining edges must have zero bends, as three bends are already used. As before, this shows that the subpath of  $\pi$  from  $v_2$  to  $u$  has rotation 0 and for  $|\text{rot}(\pi)| = 1$  it remains to show that the rotation of  $\pi$  at  $v_2$  is 0. To this end, consider the triangle  $vv_2v_3$  and the quadrangle  $v_2u_2u_3v_3$ . In the quadrangle, all edges are straight lines, which ensures that the rotation at  $v_2$  is 1. In the triangle, the rotation at  $v_2$  must also be 1 (otherwise the rotation at  $v_3$  would need to be 2, but there is no edge that can assign its bend to this  $0^\circ$  angle). Thus, the rotation of  $v_2$  in the path  $\pi$  is 0, which shows  $|\text{rot}(\pi)| = 1$ .

It follows that the path  $\pi$  has rotation 1 or  $-1$  in every Kandinsky repre-

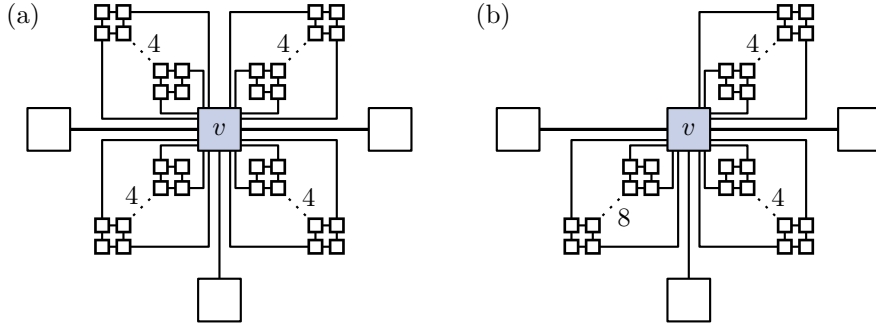


Figure 16: (a–b) A degree-3 vertex with and without fixed angles and attached corner blockers, respectively.

sentation of  $\Gamma$  that has only three bends and blocks no corner of  $v$ . Moreover, we showed that all such Kandinsky representations require three bends.  $\square$

### Putting Things Together

Let  $G = (V, E = E_0 \cup E_1)$  (together with a combinatorial embedding) be an instance of **ORTHOGONAL 01-EMBEDDABILITY**. We assume that the angles at vertices that are incident to a 1-edge are fixed. We construct an embedded graph  $G'$  that then serves as instance of **KANDINSKY BEND MINIMIZATION**. To construct  $G'$ , we start with  $G$ . Let  $v$  be a vertex incident to the face  $f$ . If the angle of  $v$  in  $f$  is fixed to  $\alpha$ , we attach  $\alpha/90^\circ$  nested corner blockers of depth 4 to  $v$  embedded next to each other into the face  $f$ ; see Figure 16a. Otherwise, if the angle is not fixed, we attach a single corner blocker of depth 4 at  $v$  in  $f$ . By suitably increasing the depth of some corner blockers we ensure that each vertex is incident to exactly 16 corner blockers; see Figure 16b. This is not strictly necessary but simplifies some of our computations. Finally, we replace every edge  $uv \in E_1$  (i.e., every edge that requires one bend) by a copy of the one-bend gadget  $\Gamma$ , identifying  $u$  and  $v$  with the endvertices of  $\Gamma$ . Note that, by assumption, both  $u$  and  $v$  have four corner blockers of depth 4. To obtain the following theorem, we show that the resulting graph  $G'$  admits a Kandinsky representation with at most  $32|V| + 3|E_1|$  bends if and only if  $G$  admits an orthogonal 01-embedding (note that deciding whether a planar embedded graph admits a Kandinsky representation with at most  $k$  bends is clearly in NP).

**Theorem 4.** **KANDINSKY BEND MINIMIZATION is NP-complete.**

*Proof.* Let  $G$  be an instance of **ORTHOGONAL 01-EMBEDDABILITY** (with fixed angles at vertices incident to 1-edges) and let  $G'$  be the corresponding instance of **KANDINSKY BEND MINIMIZATION**. Assume we have an orthogonal 01-representation  $\mathcal{O}$  of  $G$ . We show how to construct an Kandinsky representation  $\mathcal{K}$  of  $G'$  with  $32|V| + 3|E_1|$  bends. We interpret  $\mathcal{O}$  as a Kandinsky representation. We first add the nested corner blockers to the representation.

Let  $v$  be a vertex with incident face  $f$ . By construction,  $v$  has at least as many corners in  $f$  as there are nested corner blockers incident to  $v$  embedded in the face  $f$ . Thus, these corner blockers can be added with 2 bends for each corner blocker (see the drawing in Figure 13b). This yields  $32|V|$  bends in total.

Moreover, the drawings of the 1-edges can be replaced by drawings of one-bend gadgets with three bends (the drawing in Figure 15a or the symmetric drawing where the bending path  $\pi$  is bent to the other direction). This yields  $3|E_1|$  bends for all 1-edges. Hence, we get a Kandinsky representation  $\mathcal{K}$  of  $G'$  with  $32|V| + 3|E_1|$  bends in total.

For the opposite direction, we show that a Kandinsky representation  $\mathcal{K}$  of  $G'$  with at most  $32|V| + 3|E_1|$  bends implies the existence of a orthogonal 01-embedding  $\mathcal{O}$  of  $G$ . We show that the following three facts hold for  $\mathcal{K}$ .

1. Every nested corner blocker blocks a corner.
2. Every one-bend gadget has three bends and blocks no corner of its degree-3 endvertex in  $\mathcal{K}$ .
3. All remaining edges (the edges in  $E_0$ ) have 0 bends.

We use a charging argument assigning the costs for bends either to corner blockers, to one-bend gadgets or to the edges in  $E_0$ , such that the total cost is at most the total number of bends. By Lemma 8, every corner blocker of depth  $d$  requires at least  $2d$  bends. Moreover, if such a nested corner blocker does not block a corner, it has at least  $3d$  bends (Lemma 9). For corner blockers that block a corner, we charge cost  $2d$  (which is equal to the number of bends). For corner blockers blocking no corner, we charge cost  $2d + 1$  (which is  $d - 1 \geq 3$  less than the number of bends; note that all corner blockers have depth at least 4). A one-bend gadget with more than three bends is charged cost 4. A one-bend gadget that does not block a corner of its degree-3 endvertex has at least three bends by Lemma 10 and we charge cost 3 for it. If a one-bend gadget blocks a corner of its degree-3 endvertex, then at least one of the adjacent nested corner blockers does not block a corner. As we charged cost  $2d + 1$  for this corner blocker although it has at least  $3d$  bends, we can again charge cost  $3d - (2d + 1) = d - 1 \geq 3$  for the one-bend gadget. For the remaining edges in  $E_0$  we simply charge cost equal to the number of bends.

Hence, every nested corner blocker of depth  $d$  is charged at least cost  $2d$  and every one-bend gadget is charged at least cost 3. Recall that there are  $16|V|$  corner blockers and  $|E_1|$  one bend gadgets. To get a total cost of at most  $32|V| + 3|E_1|$ , every corner blocker of depth  $d$  must be charged exactly cost  $2d$ , which implies that it blocks a corner and thus shows the first fact. Since the endvertices of one-bend gadgets are incident to four corner blockers, each of which indeed blocks a corner, this also implies that no one-bend gadget can block a corner of its degree-3 endvertex. Thus, by Lemma 10, every one-bend gadget has at least three bends. Moreover, every one-bend gadget has no more than three bends as it would otherwise be charged cost 4, which shows the second fact. The third fact follows as the cost charged to edges in  $E_0$  must be 0.

By the second fact and Lemma 10 the bending path of every one-bend gadget has absolute rotation 1 in  $\mathcal{K}$ . Thus, we can replace each one-bend gadget by an edge with exactly one bend. Removing the corner blockers yields a representation of  $G$  in which no two edges leave a common incident vertex on the same side, as every nested corner blocker blocks a corner (first fact). Moreover, the edges in  $E_0$  have zero bends. Hence, the resulting representation of  $G$  is an orthogonal representation (and not only a Kandinsky representation) and the edges in  $E_1$  and  $E_0$  have one and zero bends, respectively.  $\square$

**Theorem 5.** KANDINSKY BEND MINIMIZATION is NP-complete, even if we allow empty faces or require every edge to have at most one bend (or both).

*Proof.* That the problem remains NP-hard when we require each edge to have at most one bend is obvious, as all Kandinsky representations involved in the construction above have at most one bend per edge. In fact, this requirement would even make some arguments simpler. The only place where we argued with empty faces is in the proof of Lemma 10 to exclude the situation shown in Figure 15d. It is not hard to see that this situation can also be excluded when allowing empty faces, as even in this case, it is not possible to complete the embedding without additional bends.  $\square$

## 4 A Subexponential Algorithm

In this section, we give an algorithm for computing optimal Kandinsky representations of planar graphs with fixed planar embedding in subexponential running time. To this end, we use dynamic programming on sphere cut decompositions, which are special types of branch decompositions [8].

The basic idea is as follows. Consider two graphs  $G_1$  and  $G_2$  with disjoint edge sets that share a set of *attachment vertices*. We assume that the union  $G$  of  $G_1$  and  $G_2$  is planar and has a fixed planar embedding. We say that  $G_1$  and  $G_2$  are *glueable* if both graphs are connected and there is a simple closed curve in the embedding of  $G$  that separates  $G_1$  from  $G_2$  (note that this curve must contain the attachment vertices); see Figure 17. We also say that  $G_1$  ( $G_2$ ) is a *glueable subgraph* of  $G$ .

Now assume we know two Kandinsky representations  $\mathcal{K}_1$  and  $\mathcal{K}_2$  of  $G_1$  and  $G_2$ . Depending on  $\mathcal{K}_1$  and  $\mathcal{K}_2$  one might be able to merge them into a Kandinsky representation of the whole graph  $G$ . We can generate every Kandinsky representation of  $G$  in this way, by merging every representation of  $G_1$  with every representation of  $G_2$ . Clearly, considering all pairs of representations of  $G_1$  and  $G_2$  is not efficient. Thus, we group Kandinsky representations of  $G_1$  that behave the same with respect to merging them with representations of  $G_2$  into equivalence classes. If we know an optimal Kandinsky representation for each equivalence class of  $G_1$  and  $G_2$ , it is sufficient to merge those optimal representatives of equivalence classes to obtain an optimal representation of  $G$ . If  $G$  is hierarchically decomposed, one can start with optimal Kandinsky representations of the edges and merge them step by step to obtain  $G$ .

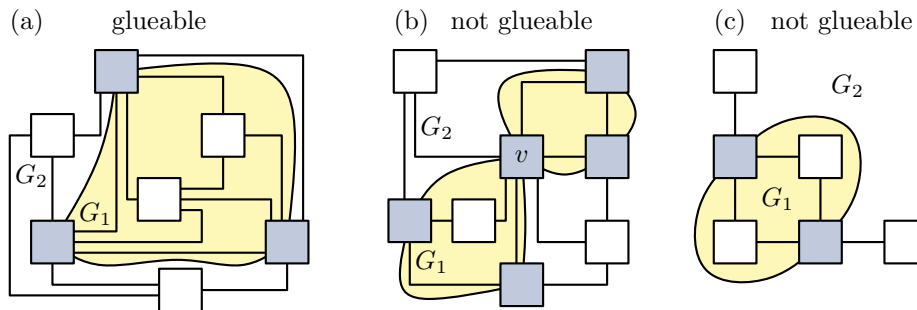


Figure 17: (a) The decomposition of a graph into two glueable subgraphs  $G_1$  and  $G_2$ . The attachment vertices are shaded blue. (b) This decomposition is not glueable, as a closed curve separating  $G_1$  from  $G_2$  cannot be simple ( $v$  must be visited twice). (c) The decomposition is not glueable since  $G_2$  is disconnected.

In the following we first characterize which Kandinsky representations of a glueable subgraph are equivalent in the sense that they can be merged with the same Kandinsky representation of the remaining graph (Section 4.1). Afterwards, we estimate in how many different ways the Kandinsky representations of subgraphs can be merged into one (Section 4.2). Finally, we conclude with the algorithm and some interesting special cases (Section 4.3).

#### 4.1 Interfaces of Kandinsky Representations

Let  $\mathcal{K}$  be a Kandinsky representation of  $G$  and let  $\mathcal{K}_1$  be the representation induced on  $G_1$ . Let  $\mathcal{K}'_1$  be another Kandinsky representation of  $G_1$ . By *replacing  $\mathcal{K}_1$  with  $\mathcal{K}'_1$  in  $\mathcal{K}$*  we mean the following. Every rotation value in  $\mathcal{K}$  involving only edges belonging to  $G_1$  are set to the value specified in  $\mathcal{K}'_1$  while all other values remain as they are. In other words the following rotations in  $\mathcal{K}$  are changed to their value in  $\mathcal{K}'_1$ :  $\text{rot}(e)$  if the edge  $e$  belongs to  $G_1$ ;  $\text{rot}(uv[u])$  and  $\text{rot}(uv[v])$  (the rotation of  $uv$  at the vertices  $u$  and  $v$ ) if  $uv$  belongs to  $G_1$ ; and  $\text{rot}(e_1, e_2)$  (for two edges  $e_1$  and  $e_2$  incident to a common vertex) if both edges  $e_1$  and  $e_2$  belong to  $G_1$ . Note that the resulting set of rotation values is not necessarily a Kandinsky representation, as some properties of Kandinsky representations might be violated.

We say that the two Kandinsky representations  $\mathcal{K}_1$  and  $\mathcal{K}'_1$  of  $G_1$  have *the same interface* if replacing  $\mathcal{K}_1$  with  $\mathcal{K}'_1$  (and vice versa) in any Kandinsky representation of  $G$  yields a Kandinsky representation of  $G$ . We will see later (Lemma 11) that it does not depend on the remaining graph  $G \setminus G_1$ , whether two representations of  $G_1$  have the same interface. The two Kandinsky representations in Figure 18a have the same interface. Clearly, having the same interface is an equivalence relation. We call the equivalence classes of this relation the *interface classes*.

Now consider again two glueable subgraphs  $G_1$  and  $G_2$  of a plane graph  $G$ . Since  $G_1$  and  $G_2$  are glueable, we know that  $G_2$  lies in a single face  $f$  of  $G_1$ .

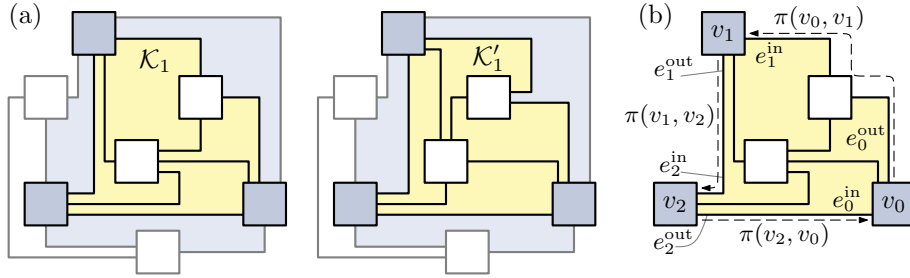


Figure 18: (a) The graph  $G$  with glueable subgraph  $G_1$  (shaded yellow). The attachment vertices and the faces shared by  $G_1$  and  $G_2$  are blue. The two Kandinsky representations  $\mathcal{K}_1$  (left) and  $\mathcal{K}'_1$  (right) of  $G_1$  are interchangeable: In any representation of  $G$  inducing  $\mathcal{K}_1$  on  $G_1$ , one can replace  $\mathcal{K}_1$  by  $\mathcal{K}'_1$  and vice versa. (b) Illustration of the notation used to define the interface paths, the attachment rotations and the  $0^\circ$  flags.

Let  $C_f$  be the facial cycle of  $f$  and assume for now, that  $C_f$  is simple (i.e.,  $G_1$  contains no cutvertex incident to  $f$ ). Let  $v_0, \dots, v_\ell$  be the attachment vertices appearing in that order in  $C_f$  (clockwise for inner, counter-clockwise for outer faces). This decomposes  $C_f$  into the paths  $\pi_f(v_0, v_1), \pi_f(v_1, v_2), \dots, \pi_f(v_\ell, v_0)$ , which we call *interface paths*. As the face we consider is unique, we often omit the subscript and simply write  $\pi(v_i, v_{i+1})$ . Moreover, the values for  $i, i-1$  and  $i+1$  are always meant modulo  $\ell+1$ . For an attachment vertex  $v_i$ , denote the last edge of the path  $\pi(v_{i-1}, v_i)$  by  $e_i^{\text{in}}$  and the first edge of the path  $\pi(v_i, v_{i+1})$  by  $e_i^{\text{out}}$ ; see Figure 18b.

Let  $\mathcal{K}_1$  and  $\mathcal{K}'_1$  be two Kandinsky representations of  $G_1$ . We say that  $\mathcal{K}_1$  and  $\mathcal{K}'_1$  have *compatible interface paths* if  $\pi(v_i, v_{i+1})$  has the same rotation in  $\mathcal{K}_1$  and  $\mathcal{K}'_1$  (i.e.,  $\text{rot}_{\mathcal{K}_1}(\pi(v_i, v_{i+1})) = \text{rot}_{\mathcal{K}'_1}(\pi(v_i, v_{i+1}))$ ) for every  $i = 1, \dots, k$ . Moreover,  $\mathcal{K}_1$  and  $\mathcal{K}'_1$  have *the same attachment rotations* if for every attachment vertex  $v_i$ , the rotation  $\text{rot}(e_i^{\text{in}}, e_i^{\text{out}})$  is the same in  $\mathcal{K}_1$  and  $\mathcal{K}'_1$ . In Figure 18b, the interface paths  $\pi(v_0, v_1)$ ,  $\pi(v_1, v_2)$ , and  $\pi(v_2, v_0)$  have rotations  $-1, 1$ , and  $0$ , respectively, and the attachment rotations at the vertices  $v_0, v_1$ , and  $v_2$  are  $-1, -1$ , and  $-2$ , respectively.

When considering orthogonal representations (with maximum degree 4) and not Kandinsky representations, having compatible interface paths and the same attachment rotations is sufficient for two representations to have the same interface. In case of Kandinsky representations, we have to care about  $0^\circ$  angles at the attachment vertices. Thus, for an attachment vertex  $v_i$ , the rotations at the end  $v_i$  of the edges  $e_i^{\text{in}}$  and  $e_i^{\text{out}}$  ( $\text{rot}(e_i^{\text{in}}[v_i])$  and  $\text{rot}(e_i^{\text{out}}[v_i])$ ), which can take the values  $-1, 0$ , or  $1$  are of importance. The actual value of these rotations is not important, we only care about whether they are  $-1$  or something else. We call these information the  $0^\circ$  flags, which has the value **true** for a rotation of  $-1$  and **false** otherwise. We say that  $\mathcal{K}_1$  and  $\mathcal{K}'_1$  have *the same  $0^\circ$  flags* if all their  $0^\circ$  flags have the same values. Possible values for the  $0^\circ$  flags in Figure 18b

are **true** for  $e_0^{\text{out}}[v_0]$  and for  $e_1^{\text{in}}[v_1]$  and **false** for all other flags.

In case the facial cycle  $C_f$  is not simple, it might contain an attachment vertex  $v_i$  several times. However, since  $G_1$  and  $G_2$  are glueable, the simple closed curve separating  $G_1$  from  $G_2$  gives an order of the attachment vertices. We simply take this order to define the interface paths. All remaining definitions work as before.

**Lemma 11.** *Two Kandinsky representations have the same interface if and only if they have compatible interface paths, the same attachment rotations, and the same  $0^\circ$  flags.*

*Proof.* We first show the only-if part. Let  $G$  be a plane graph with Kandinsky representation  $\mathcal{K}$  with restriction  $\mathcal{K}_1$  to the glueable subgraph  $G_1$ . Let  $\mathcal{K}'_1$  be another Kandinsky representation of  $G_1$ . Assume there is an interface path  $\pi$  that has a different rotation in  $\mathcal{K}_1$  than in  $\mathcal{K}'_1$ . Let  $f$  be the face incident to  $\pi$  shared by  $G_1$  and the remaining graph  $G_2$  (one of the blue faces in Figure 18a). By replacing  $\mathcal{K}_1$  with  $\mathcal{K}'_1$  the rotation of  $\pi$  in  $f$  changes, but all other rotations in  $f$  stay the same. Thus, the total rotation around  $f$  cannot be 4 ( $-4$  if  $f$  is the outer face), which shows that the resulting set of rotations is not a Kandinsky representation of  $G$  (contradiction to Property (1)). Hence,  $\mathcal{K}_1$  and  $\mathcal{K}'_1$  do not have the same interface. A similar argument shows that having the same attachment rotations is necessary, since otherwise the total rotation around a vertex would change by replacing  $\mathcal{K}_1$  with  $\mathcal{K}'_1$ , which contradicts Property (3).

Finally, assume  $\mathcal{K}_1$  and  $\mathcal{K}'_1$  have different  $0^\circ$  flags. Thus, there exists an attachment vertex  $v$  with incident edge  $e_1$  (belonging to an interface path) such that  $\text{rot}(e_1[v])$  is (without loss of generality)  $-1$  in  $\mathcal{K}_1$  (value **true**) and 0 or 1 in  $\mathcal{K}'_1$  (value **false**). As  $v$  is an attachment vertex, the remaining graph  $G_2$  contains an edge incident to  $v$ . Let  $e_2$  be the edge of  $G_2$  incident to  $v$  that shares a face  $f$  with  $e_1$ . Then one might choose the Kandinsky representation  $\mathcal{K}$  of  $G$  such that the rotation  $\text{rot}_f(e_1, e_2)$  at  $v$  in  $f$  is 2 (angle of  $0^\circ$ ) while  $\text{rot}_f(e_2[v])$  is 0 or 1. Then  $\text{rot}(e_1[v])$  must be  $-1$  by Property (5), which is true for  $\mathcal{K}_1$  but not for  $\mathcal{K}'_1$ . Hence, replacing  $\mathcal{K}_1$  with  $\mathcal{K}'_1$  does not yield a Kandinsky representation of  $G$ , which shows that having the same  $0^\circ$  flags is also necessary for having the same interface.

For the other direction, let  $G_1$  and  $G_2$  be glueable graphs with union  $G$  and let  $\mathcal{K}$  be a Kandinsky representation of  $G$  with restrictions  $\mathcal{K}_1$  and  $\mathcal{K}_2$  to  $G_1$  and  $G_2$ , respectively. Let  $\mathcal{K}'_1$  be a Kandinsky representation of  $G_1$  with compatible interface paths, the same attachment rotations, and the same  $0^\circ$  flags. We show that replacing  $\mathcal{K}_1$  with  $\mathcal{K}'_1$  in  $\mathcal{K}$  yields a Kandinsky representation of  $G$  by showing that the resulting rotation values satisfy properties (1)–(5) from Section 2.2.

Property (2) is trivially satisfied, as all rotations concerning a single edge come either from  $\mathcal{K}'_1$  or from  $\mathcal{K}_2$ , which are both Kandinsky representations and thus satisfy this property. Property (4) is also satisfied, as the rotation at a vertex either stays as it is in  $\mathcal{K}$  or it is changed to its value in  $\mathcal{K}'_1$  and thus lies in the interval  $[-2, 2]$ .

For Property (1), consider a face  $f$  of  $G$ . If all edges in the boundary of  $f$  belong to only one of the graphs  $G_1$  and  $G_2$ , then the total rotation in  $f$  is equal to its total rotation in  $\mathcal{K}'_1$  or  $\mathcal{K}_2$ , respectively. As  $\mathcal{K}'_1$  and  $\mathcal{K}_2$  are Kandinsky representations, they satisfy Property (1). If the boundary of  $f$  contains edges from both graphs  $G_1$  and  $G_2$  (one of the blue faces in Figure 18a), it is composed of two interface paths  $\pi_1$  and  $\pi_2$  belonging to  $G_1$  and  $G_2$ , respectively, that share their endvertices  $u$  and  $v$ . By replacing  $\mathcal{K}_1$  with  $\mathcal{K}'_1$ , the representation of  $\pi_2$  does not change. Moreover, the rotations at  $u$  and  $v$  in  $f$  remain unchanged. The representation of  $\pi_1$  might of course change, however, the rotation remains the same as  $\mathcal{K}_1$  and  $\mathcal{K}'_1$  have compatible interface paths.

A similar argument shows that Property (5) is satisfied. Let  $v$  be a vertex with rotation 2 (corresponding to an angle of  $0^\circ$ ) in a face  $f$ , i.e.,  $\text{rot}_f(uv, vw) = 2$ . We only need to consider the case where (without loss of generality)  $uv$  belongs to  $G_1$  and  $vw$  belongs to  $G_2$ , as all other cases are trivial. Then  $\text{rot}_f(uv[v]) = -1$  or  $\text{rot}_f(vw[v]) = -1$  holds in  $\mathcal{K}$ . In the latter case,  $\text{rot}_f(vw[v])$  does not change by replacing  $\mathcal{K}_1$  with  $\mathcal{K}'_1$  as  $vw$  belongs to  $G_2$ . In the former case,  $\text{rot}_f(uv[v]) = -1$  implies that the corresponding  $0^\circ$  flag in  $\mathcal{K}_1$  is **true**. As  $\mathcal{K}_1$  and  $\mathcal{K}'_1$  have the same  $0^\circ$  flags, this flag is also **true** in  $\mathcal{K}'_1$ , which implies that  $\text{rot}_f(uv[v]) = -1$  is still true in  $\mathcal{K}'_1$  and thus in  $\mathcal{K}'$ .

Finally, to show Property (3), consider a vertex  $v$ . If  $v$  is not an attachment vertex, all rotations at  $v$  come either from  $\mathcal{K}'_1$  or from  $\mathcal{K}_2$  and thus satisfy Property (3). Let  $v$  be an attachment vertex and let  $f_1$  be the face of  $G_1$  that completely contains  $G_2$ . The only rotations at  $v$  that might change by replacing  $\mathcal{K}_1$  with  $\mathcal{K}'_1$  are the rotations in faces not shared with  $G_2$ . These are exactly the faces of  $G_1$  incident to  $v$  except for  $f_1$ . As  $\mathcal{K}_1$  and  $\mathcal{K}'_1$  have the same rotations at attachment vertices, the rotation  $\text{rot}_{f_1}(v)$  is the same in  $\mathcal{K}_1$  and  $\mathcal{K}'_1$ . Thus, by Property (3) the sum of all other rotations around  $v$  in  $G_1$  must also be the same in both representations  $\mathcal{K}_1$  and  $\mathcal{K}'_1$ . Hence, the total sum of rotations at  $v$  does not change by replacing  $\mathcal{K}_1$  with  $\mathcal{K}'_1$ , which concludes the proof.  $\square$

It follows that each interface class is uniquely described by the rotations of the interface paths, by the rotations at the attachment vertices, and by the values of the  $0^\circ$  flags. We simply call this set of information the *interface* of  $G_1$  ( $G_2$ ) in  $G$ . Note that this redefines what it means for two Kandinsky representations to have the same interface. However, the definitions are consistent due to Lemma 11 and we will use them interchangeably.

## 4.2 Merging two Kandinsky Representations

So far, we considered the case that there is a Kandinsky representation  $\mathcal{K}$  of  $G$  that can be altered by replacing the Kandinsky representation of the subgraph  $G_1$ . Now we change the point of view and assume we have Kandinsky representations  $\mathcal{K}_1$  and  $\mathcal{K}_2$  of  $G_1$  and  $G_2$ , respectively, that we want to combine to get a Kandinsky representation of  $G$ . We say that  $\mathcal{K}_1$  and  $\mathcal{K}_2$  can be *merged* if there exists a Kandinsky representation  $\mathcal{K}$  of  $G$  whose restriction to  $G_1$  and  $G_2$  is  $\mathcal{K}_1$  and  $\mathcal{K}_2$ , respectively. Note that the only rotations in  $\mathcal{K}$  that occur neither in  $\mathcal{K}_1$

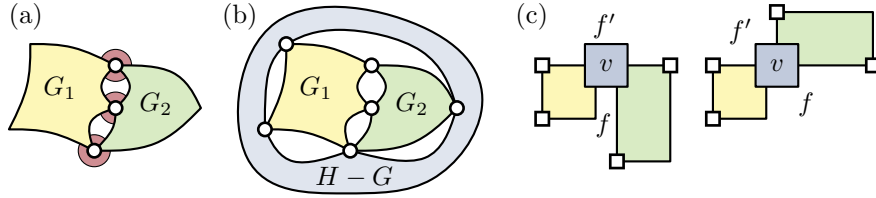


Figure 19: (a) Merging  $G_1$  and  $G_2$ . The shared rotations are marked red. (b) Illustration of a merging step. The width of this merging step is 5 ( $G_1$  has 5 attachment vertices). (c) Two ways to choose the shared rotations.

nor in  $\mathcal{K}_2$  are rotations at attachment vertices between an edge of  $G_1$  and an edge of  $G_2$ . We call these rotations the *shared rotations*; see Figure 19a. Thus, merging  $\mathcal{K}_1$  and  $\mathcal{K}_2$  is the process of choosing values for the shared rotation, such that the resulting set of rotations is a Kandinsky representation of  $G$ .

In the following, we consider the case where  $G$  itself is a glueable subgraph of a larger graph  $H$ . We call this the *merging step*  $G = G_1 \sqcup G_2$ . Note that  $G_1$  and  $G_2$  are not only glueable subgraphs of  $G$  but also of  $H$ . Note further that the interface of  $G_1$  ( $G_2$ ) in  $G$  can be deduced from the interface of  $G_1$  ( $G_2$ ) in  $H$ . When dealing with a merging step, we always consider the interfaces of  $G_1$  and  $G_2$  in  $H$  (which contain more information than their interfaces in  $G$ ). The *width* of a merging step is the maximum number of attachment vertices of  $G_1$ ,  $G_2$ , and  $G$  in  $H$ ; see Figure 19b for an example.

If the Kandinsky representations  $\mathcal{K}_1$  and  $\mathcal{K}_2$  can be merged, then every Kandinsky representation  $\mathcal{K}'_1$  with the same interface as  $\mathcal{K}_1$  can be merged in the same way (i.e., with the same shared rotations) with  $\mathcal{K}_2$  as one can first merge  $\mathcal{K}_1$  with  $\mathcal{K}_2$  and then replace  $\mathcal{K}_1$  by  $\mathcal{K}'_1$ . Moreover, the resulting Kandinsky representations  $\mathcal{K}$  and  $\mathcal{K}'$  of  $G$  have the same interface for the following reason. In every Kandinsky representation of  $H$  the representation  $\mathcal{K}$  can be replaced by  $\mathcal{K}'$  as this is equivalent to replacing  $\mathcal{K}_1$  by  $\mathcal{K}'_1$  (which can be done as  $\mathcal{K}_1$  and  $\mathcal{K}'_1$  have the same interface). Thus, the only choices that matter when merging two Kandinsky representations are to choose shared rotations and interfaces for  $G_1$  and  $G_2$ . Thus, the term of merging Kandinsky representations extends to *merging interfaces*. We call a choice of shared rotations and interfaces for  $G_1$  and  $G_2$  *compatible*, if these interfaces can be merged using the chosen rotations.

The following lemma bounds the number of compatible combinations. It is parametrized with the width  $k$  of the merging step and the *maximum rotation*  $\rho$ . The maximum rotation of a graph  $H$  is  $\rho$  if  $H$  admits an optimal Kandinsky representation such that the absolute rotations of the interface paths in every glueable subgraph of  $H$  are at most  $\rho$ . With the maximum rotation of a merging step, we mean the maximum rotation of the whole graph  $H$ . We give bounds for  $\rho$  in Lemma 14.

**Lemma 12.** *In a merging step  $G = G_1 \sqcup G_2$  of width  $k$  with maximum rotation  $\rho$ , there are at most  $(2\rho + 1)^{\lfloor 1.5k \rfloor - 1} \cdot 330^k$  compatible choices for the shared rotations and the interfaces of  $G_1$  and  $G_2$ .*

*Proof.* Let  $k_{12}$  be the number of attachment vertices shared by  $G_1$  and  $G_2$  and let  $k_1$  and  $k_2$  be the number of exclusive attachment vertices of  $G_1$  and  $G_2$ , respectively. In the example in Figure 19b,  $k = 5$ ,  $k_{12} = 3$ ,  $k_1 = 2$ , and  $k_2 = 1$ . As  $G_1$  and  $G_2$  both have at most  $k$  attachment vertices, we have  $k_1 + k_{12} \leq k$  and  $k_2 + k_{12} \leq k$ . Moreover, every exclusive attachment vertex is an attachment vertex of  $G$ , thus  $k_1 + k_2 \leq k$  holds. By summing these three inequalities we directly get  $k_1 + k_2 + k_{12} \leq \lfloor 1.5k \rfloor$ . We start with a rough estimation of the possible combinations and then show how to reduce the number by ruling out choices that are not compatible and thus will never lead to a Kandinsky representation.

The graph  $G_1$  has  $k_1 + k_{12} \leq k$  attachment vertices and thus also  $k_1 + k_{12} \leq k$  interface paths. The absolute rotation of each interface path is at most  $\rho$ , thus there are at most  $2\rho + 1$  possible values for those rotations. This leads to at most  $(2\rho + 1)^k$  combinations. For every attachment vertex there is the attachment rotation that can be any of the five integers in  $[-2, 2]$ . Moreover, there are two binary  $0^\circ$  flags for each attachment vertex which gives  $5 \cdot 2 \cdot 2 = 20$  possible configurations for each attachment vertex. Thus, there are up to  $20^k$  combinations for the  $k_1 + k_{12} \leq k$  attachment vertices in  $G_1$ . We get the same bounds for  $G_2$ . Hence, there are at most  $(2\rho + 1)^{2k} \cdot 400^k$  combinations for choosing an interface for  $G_1$  and  $G_2$ . For every shared attachment vertex, there are two shared rotations we need to set, which gives 25 combinations as these rotations can take values in  $[-2, 2]$ . For the  $k_{12}$  shared rotations, this gives  $25^{k_{12}} \leq 25^k$  combinations, which makes  $(2\rho + 1)^{2k} \cdot 10000^k$  combinations in total.

We start with the exponent in the factor  $(2\rho + 1)^{2k}$ . The exponent  $2k$  came from the fact that we chose rotations of  $k_1 + k_{12} + k_2 + k_{12}$  interface paths. Assume we have fixed the interface of  $G_1$  except for the rotation of a single interface path. As the total rotation around the face bounded by the interface paths is 4 ( $-4$  for the outer face) in every Kandinsky representation, there is no choice left for the rotation of this path. Thus, we only have to choose the rotation of  $k_1 + k_{12} - 1$  interface paths in  $G_1$ . The same holds for  $G_2$ , which gives  $k_1 + k_{12} + k_2 + k_{12} - 2$  interface paths in total. As there are  $k_{12}$  shared attachment vertices, the graph  $G$  has  $k_{12} - 1$  faces that are bounded by one interface path of  $G_1$  and one interface path of  $G_2$ . Assume the rotation of the interface paths of  $G_1$  is fixed and the shared rotations are fixed. Then the rotations of these  $k_{12} - 1$  interface paths of  $G_2$  are also fixed as the rotation around these faces must sum to 4 ( $-4$ ). Thus, there are  $k_{12} - 1$  additional interface paths whose rotation is automatically fixed. Hence, we get the exponent down to  $k_1 + k_2 + k_{12} - 1$  which is at most  $\lfloor 1.5k \rfloor - 1$ .

To reduce the basis of the  $10000^k$  factor, first note that some configurations of choosing attachment rotations and  $0^\circ$  flags are not possible. Let  $f$  be the face of  $G_1$  containing all attachment vertices and let  $v$  be an attachment vertex. Let  $e^{\text{in}}$  and  $e^{\text{out}}$  be the two edges incident to  $v$  and  $f$ , i.e.,  $\text{rot}_f(e^{\text{in}}, e^{\text{out}})$  is the attachment rotation at  $v$ . Assume  $\text{rot}_f(e^{\text{in}}, e^{\text{out}}) = 2$ , i.e., there is an angle of  $0^\circ$  at  $v$ . Due to Property (5),  $e^{\text{in}}$  or  $e^{\text{out}}$  must have a rotation of  $-1$  at the vertex  $v$  in  $f$  ( $\text{rot}_f(e^{\text{in}}[v]) = -1$  or  $\text{rot}_f(e^{\text{out}}[v]) = -1$ ). Thus if the attachment

rotation at  $v$  is 2, at least one of the two  $0^\circ$  flags at  $v$  must be **true**. A similar argument shows that an attachment rotation of  $-2$  at  $v$  implies that at least one of the  $0^\circ$  flags at  $v$  is **false**. Thus, there are only 18 (instead of 20) possibilities for choosing the attachment rotation and the  $0^\circ$  flags at an attachment vertex. Thus, for the exclusive attachment vertices in  $G_1$  and  $G_2$  we get  $18^{k_1+k_2}$  combinations. Moreover, we have  $18^{2k_{12}}$  combinations for the shared attachment vertices in  $G_1$  and  $G_2$  and  $25^{k_{12}}$  combinations for the shared rotations.

We show that not all these  $18^{2k_{12}} \cdot 25^{k_{12}}$  need to be considered. Let  $v$  be a shared attachment vertex and let  $\text{rot}_1$  and  $\text{rot}_2$  be the attachment rotations for  $v$  in  $G_1$  and  $G_2$ , respectively. Let further  $f$  and  $f'$  be the two faces incident to  $v$  shared by  $G_1$  and  $G_2$  and let  $\text{rot}_f$  and  $\text{rot}_{f'}$  be the corresponding shared rotations at  $v$  in  $f$  and  $f'$ . Finally, let  $x_f$  ( $x_{f'}$ ) be a variable with the value 1 if the  $0^\circ$  flags do not allow a  $0^\circ$  angle in  $f$  ( $f'$ ) and the value 0 if they allow a  $0^\circ$  angle, which is the case if and only if at least one of the corresponding flags is **true**. It is not hard to see, that fixing the attachment rotations  $\text{rot}_1$  and  $\text{rot}_2$  and the  $0^\circ$  flags leaves  $-\text{rot}_1 - \text{rot}_2 + 1 - x_f - x_{f'}$  possible combinations (or 0 if this value is negative) to set the shared rotations when the result must obey the properties of a Kandinsky representation. In Figure 19c,  $\text{rot}_1 = -1$  and  $\text{rot}_2 = -1$  holds. The  $0^\circ$  flags allow for a  $0^\circ$  angle in  $f$  but not in  $f'$ , thus  $x_f = 0$  and  $x_{f'} = 1$ . This leaves only two ways to fix the shared rotations, namely  $\text{rot}_f = 2$ ,  $\text{rot}_{f'} = 0$  and  $\text{rot}_f = 1$ ,  $\text{rot}_{f'} = 1$ . Counting those combinations for each of the 18 ways to fix the interface rotations and  $0^\circ$  flags of  $v$  in  $G_1$  and  $G_2$  (which can be done with a simple computer program) results in 330 combinations. Thus, the  $18^{2k_{12}} \cdot 25^{k_{12}}$  combinations for the shared attachment vertices reduce to  $330^{k_{12}}$ . Hence, there are at most  $18^{k_1+k_2} \cdot 330^{k_{12}}$  combinations for choosing attachment rotations,  $0^\circ$  flags, and shared rotations. Note that  $18^2 = 324 \leq 330$  and thus we get the following.

$$18^{k_1+k_2} \cdot 330^{k_{12}} \leq \sqrt{330}^{k_1+k_2} \cdot \sqrt{330}^{2k_{12}} = \sqrt{330}^{k_1+k_{12}+k_2+k_{12}} \leq \sqrt{330}^{2k} = 330^k$$

To conclude, we get at most  $330^k$  possibilities to choose all attachment rotations, all  $0^\circ$  flags, and all shared rotations. Once those are chosen, at most  $(2\rho+1)^{\lfloor 1.5k \rfloor - 1}$  ways to choose rotations of the interface paths remain. Note that it is easy to list these combinations efficiently (without considering unnecessary combinations).  $\square$

Let  $G$  be a glueable subgraph of  $H$ . The *cost* of an interface class is the minimum cost of the Kandinsky representations it contains (recall that an interface class is a set of Kandinsky representations that have the same interface). The *cost table* of  $G$  is a table containing the cost of each interface class of  $G$ .

**Lemma 13.** *Let  $G = G_1 \sqcup G_2$  be a merging step of width  $k$  with maximum rotation  $\rho$ . Given the cost tables of  $G_1$  and  $G_2$ , the cost table of  $G$  can be computed on  $O(k \cdot (2\rho+1)^{\lfloor 1.5k \rfloor - 1} \cdot 330^k)$  time.*

*Proof.* Start with a cost table for  $G$  with cost  $\infty$  for every interface class. We iterate over all  $(2\rho+1)^{\lfloor 1.5k \rfloor - 1} \cdot 330^k$  compatible choices for the shared rotations

and the interfaces of  $G_1$  and  $G_2$  (Lemma 12). Consider a fixed choice and let  $[\mathcal{K}_1]$  and  $[\mathcal{K}_2]$  be the chosen interface classes of  $G_1$  and  $G_2$  with cost  $c_1$  and  $c_2$ . In  $O(k)$  time we can compute the interface class  $[\mathcal{K}]$  we get for  $G$ . If  $c_1 + c_2$  is less than the current cost  $[\mathcal{K}]$ , we set it to  $c_1 + c_2$ .

Note that the cost  $c_1$  and  $c_2$  imply the existence of Kandinsky representations  $\mathcal{K}'_1 \in [\mathcal{K}_1]$  and  $\mathcal{K}'_2 \in [\mathcal{K}_2]$  with cost  $c_1$  and  $c_2$ . These two Kandinsky representations can be merged (using the fixed shared rotations) to a Kandinsky representation  $\mathcal{K}' \in [\mathcal{K}]$ . This representation clearly has cost  $c_1 + c_2$  and thus the cost of  $[\mathcal{K}]$  is at most  $c_1 + c_2$ .

On the other hand, assume that there exists a Kandinsky representation  $\mathcal{K}$  of  $G$  with cost  $c$ . Let  $\mathcal{K}_1$  and  $\mathcal{K}_2$  be the restrictions of  $\mathcal{K}$  to  $G_1$  and  $G_2$ , respectively. Let further  $c_1$  and  $c_2$  be the costs of  $\mathcal{K}_1$  and  $\mathcal{K}_2$ , respectively. Then  $c = c_1 + c_2$  holds. Moreover, the costs of the equivalence classes  $[\mathcal{K}_1]$  and  $[\mathcal{K}_2]$  are  $c'_1 \leq c_1$  and  $c'_2 \leq c_2$ , respectively. As  $[\mathcal{K}_1]$  and  $[\mathcal{K}_2]$  can be merged to  $[\mathcal{K}]$ , at some point we set the cost of  $[\mathcal{K}]$   $c'_1 + c'_2 \leq c_1 + c_2 = c$ . Thus, on one hand, the cost of each equivalence class  $[\mathcal{K}]$  of  $G$  is never set to something below its actual cost, and on the other hand it is at some point set to a value that is at most its actual cost. Hence, this procedure yields the cost table of  $G$ .  $\square$

### 4.3 The Algorithm

The previous three lemmas together with a dynamic program on a sphere cut decomposition (which is a special type of branch decomposition) yield the following theorem.

**Theorem 6.** *An optimal Kandinsky representation of a plane graph  $G$  can be computed in  $O(n^3 + n \cdot k \cdot (2\rho + 1)^{\lceil 1.5k \rceil - 1} \cdot 330^k)$  time, where  $k$  is the branch width and  $\rho$  the maximum rotation of  $G$ .*

*Proof.* Let  $H$  be the plane graph. If  $H$  contains a degree-1 vertex, we can attach a cycle of length 4 to it. Computing an optimal Kandinsky representation of the resulting graph and removing this cycle from it obviously gives an optimal Kandinsky representation of  $H$ . Thus, we can assume without loss of generality that  $H$  does not contain degree-1 vertices.

In planar graphs, a branch decomposition with minimum width can be computed in polynomial [18] and even  $O(n^3)$  [15] time. Moreover, Dorn et al. [8, Theorem 1] show that one can compute a sphere cut decomposition of width  $k$  from a given branch decomposition of width  $k$  in  $O(n^3)$  time, if  $G$  does not contain degree-1 vertices. Without defining sphere cut decomposition precisely, it is essentially a rooted binary tree  $\mathcal{T}$  (every node has two children or is a leaf) with a bijection between the edges of  $H$  and the leaves of  $\mathcal{T}$  such that the following property holds. For every node  $\mu$  of  $\mathcal{T}$ , the edges of  $H$  corresponding to leaves that are ancestors of  $\mu$  induce a glueable subgraph of  $H$ . Denote this subgraph by  $G_\mu$ .

Clearly, this implies that for an inner node  $\mu$  with children  $\mu_1$  and  $\mu_2$ , we get a merging step  $G_\mu = G_{\mu_1} \sqcup G_{\mu_2}$ . We process the inner nodes of  $\mathcal{T}$  bottom up to compute the cost table of  $G_\mu$  for every node  $\mu$ . If a child  $\mu_i$  (for  $i = 1, 2$ ) of

$\mu$  is a leaf, it corresponds to a single edge for which the cost tables are trivially known. Otherwise, we already processed the child  $\mu_i$  and thus know the cost table of  $G_{\mu_i}$ . Hence, by Lemma 13, we can compute the cost table of  $G_\mu$  in  $O(k \cdot (2\rho + 1)^{\lfloor 1.5k \rfloor - 1} \cdot 330^k)$  time. Doing this for every inner node of  $\mathcal{T}$  gives the claimed running time, since  $\mathcal{T}$  contains  $O(n)$  inner nodes. Moreover, for the root  $\tau$ , we have  $G_\tau = H$ . Thus, after processing the root  $\tau$ , we know the cost of an optimal Kandinsky representation of  $H$ . To actually compute an optimal Kandinsky representation of  $H$  (and not only its cost) one simply has to track the interface classes that lead to the optimal solution through the dynamic program.  $\square$

We get the following bounds for the maximum rotation  $\rho$  of a graph.

**Lemma 14.** *Let  $G$  be a graph with Kandinsky representation  $\mathcal{K}$ . Let  $\Delta_F$  be the maximum face degree of  $G$  and let  $\rho$  be the maximum absolute rotation of interface paths of glueable subgraphs of  $G$ . The following holds.*

- $\rho \leq m + \Delta_F - 2$ , if  $\mathcal{K}$  is an optimal Kandinsky representation.
- $\rho \leq (b + 1) \cdot \Delta_F - b - 2$ , if  $\mathcal{K}$  is a  $b$ -bend Kandinsky representation.

*Proof.* First note that every interface path of a glueable subgraph is a subpath of a face of  $G$ . Thus, interface paths have length at most  $\Delta_F - 1$ . We show that the maximum rotation of a path of this length satisfies the claimed bounds. Proving that the absolute value of the minimum rotation also satisfies these bounds is symmetric.

Consider the case that  $\mathcal{K}$  is an optimal Kandinsky representation. As  $G$  admits a 1-bend representation [12], there exists a representation with  $m$  bends and an optimal representation  $\mathcal{K}$  has at most  $m$  bends. Thus, the edges on the interface path have at most  $m$  bends contributing rotation at most  $m$ . An interface path of length (in terms of number of edges) at most  $\Delta_F - 1$  has at most  $\Delta_F - 2$  inner vertices. If the rotation of each inner vertex is at most 1 we get the claimed inequality  $\rho \leq m + \Delta_F - 2$ . Consider a vertex  $v$  with rotation 2. Due to Property (5), at least one of the two edges in the path incident to  $v$  must have rotation  $-1$ . Thus, we can account rotation 1 even for vertices with rotation 2, yielding  $\rho \leq m + \Delta_F - 2$ .

In case  $\mathcal{K}$  is a  $b$ -bend Kandinsky representation, the rotation contributed by the edges is at most  $b \cdot (\Delta_F - 1)$ . Together with the  $\Delta_F - 2$  upper bound for the vertices, this gives  $\rho \leq b \cdot \Delta_F - b + \Delta_F - 2 = (b + 1) \cdot \Delta_F - b - 2$ .  $\square$

We get the following corollaries by plugging the bounds of Lemma 14 into Theorem 6, using that the branch width of series-parallel graphs is 2, and that the branch width of planar graphs is in  $O(\sqrt{n})$  (in fact, the branch width of a planar graph is at most  $2.122\sqrt{n}$  [11]).

**Corollary 2.** *Let  $G$  be a plane graph with maximum face-degree  $\Delta_F$ , and branch width  $k$ . An optimal Kandinsky representation can be computed in  $O(n^3 + n \cdot k \cdot (2m + 2\Delta_F - 3)^{\lfloor 1.5k \rfloor - 1} \cdot 330^k)$  time. An optimal  $b$ -bend Kandinsky representation can be computed in  $O(n^3 + n \cdot k \cdot ((2b + 2) \cdot \Delta_F - 2b - 3)^{\lfloor 1.5k \rfloor - 1} \cdot 330^k)$  time.*

**Corollary 3.** *For series-parallel graphs an optimal Kandinsky representation can be computed in  $O(n^3)$  time.*

**Corollary 4.** *For plane graphs an optimal Kandinsky representation can be computed in  $2^{O(\sqrt{n} \log n)}$  time.*

## 5 Conclusion

In this paper we have shown that bend minimization in the Kandinsky model is NP-complete, thus answering a question that was open for almost two decades. The proof also extends to the case that every edge may have at most one bend and for the case that empty faces are allowed.

On the positive side, we gave an algorithm with running time  $2^{O(k \log n)}$  for graphs of bounded branch width. In fact, the problem is FPT with respect to  $k + b + \Delta_F$ , where  $k$  is the branch width,  $b$  is the maximum number of bends on a single edge in the drawing and  $\Delta_F$  is the size of the largest face in the combinatorial embedding. For general planar graphs this gives a subexponential exact algorithm with running time  $2^{O(\sqrt{n} \log n)}$ .

We leave open the question whether the number of parameters used to obtain an FPT algorithm can be decreased. Is the problem  $W[1]$ -hard when parameterized by branch width only?

**Acknowledgments.** We thank Therese Biedl for discussions.

## References

- [1] P. Bertolazzi, G. Di Battista, and W. Didimo. Computing orthogonal drawings with the minimum number of bends. *IEEE Transactions on Computers*, 49(8):826–840, 2000.
- [2] T. Biedl and G. Kant. A better heuristic for orthogonal graph drawings. *Computational Geometry: Theory and Applications*, 9:159–180, 1998.
- [3] T. Bläsius, M. Krug, I. Rutter, and D. Wagner. Orthogonal graph drawing with flexibility constraints. *Algorithmica*, 68(4):859–885, 2014.
- [4] T. Bläsius, S. Lehmann, and I. Rutter. Orthogonal graph drawing with inflexible edges. *CoRR*, abs/1404.2943, 2014.
- [5] T. Bläsius, I. Rutter, and D. Wagner. Optimal orthogonal graph drawing with convex bend costs. In F. V. Fomin, R. Freivalds, M. Kwiatkowsak, and D. Peleg, editors, *Proceedings of the 40th International Colloquium on Automata, Languages and Programming (ICALP’13)*, volume 7965 of *Lecture Notes in Computer Science*, pages 184–195. Springer Berlin/Heidelberg, 2013.

- [6] S. Cornelsen and A. Karrenbauer. Accelerated bend minimization. *Journal of Graph Algorithms and Applications*, 16(3):635–650, 2012.
- [7] M. de Berg and A. Khosravi. Optimal binary space partitions for segments in the plane. *International Journal of Computational Geometry & Applications*, 22(3):187–206, 2012.
- [8] F. Dorn, E. Penninkx, H. Bodlaender, and F. Fomin. Efficient exact algorithms on planar graphs: Exploiting sphere cut decompositions. *Algorithmica*, 58(3):790–810, 2010.
- [9] M. Eiglsperger. *Automatic Layout of UML Class Diagrams: A Topology-Shape-Metrics Approach*. PhD thesis, Universität Tübingen, 2003.
- [10] M. Eiglsperger, C. Gutwenger, M. Kaufmann, J. Kupke, M. Jünger, S. Leipert, K. Klein, P. Mutzel, and M. Siebenhaller. Automatic layout of UML class diagrams in orthogonal style. *Information Visualization*, 3(3):189–208, 2004.
- [11] F. V. Fomin and D. M. Thilikos. New upper bounds on the decomposability of planar graphs. *Journal of Graph Theory*, 51(1):53–81, 2006.
- [12] U. Fößmeier, G. Kant, and M. Kaufmann. 2-visibility drawings of planar graphs. In S. North, editor, *Proceedings of the 5th International Symposium on Graph Drawing (GD'96)*, volume 1190 of *Lecture Notes in Computer Science*, pages 155–168. Springer Berlin/Heidelberg, 1997.
- [13] U. Fößmeier and M. Kaufmann. Drawing high degree graphs with low bend numbers. In F. J. Brandenburg, editor, *Proceedings of the 4th International Symposium on Graph Drawing (GD'95)*, volume 1027 of *Lecture Notes in Computer Science*, pages 254–266. Springer Berlin/Heidelberg, 1995.
- [14] A. Garg and R. Tamassia. On the computational complexity of upward and rectilinear planarity testing. *SIAM Journal on Computing*, 31(2):601–625, 2001.
- [15] Q.-P. Gu and H. Tamaki. Optimal branch-decomposition of planar graphs in  $O(n^3)$  time. *ACM Transactions on Algorithms*, 4(3):30:1–30:13, 2008.
- [16] G. W. Klau and P. Mutzel. Quasi-orthogonal drawing of planar graphs. Research Report MPI-I-98-1-013, Max-Planck-Institut für Informatik, 1998.
- [17] C. E. Leiserson. Area-efficient graph layouts (for VLSI). In *Proceedings of the IEEE 21st Annual Symposium on Foundations of Computer Science (FOCS'80)*, pages 270–281, 1980.
- [18] P. Seymour and R. Thomas. Call routing and the ratcatcher. *Combinatorica*, 14(2):217–241, 1994.
- [19] R. Tamassia. On embedding a graph in the grid with the minimum number of bends. *SIAM Journal on Computing*, 16(3):421–444, 1987.

- [20] R. Tamassia, editor. *Handbook of Graph Drawing and Visualization*. Number 81 in Discrete Mathematics and Its Applications. Chapman and Hall/CRC, 2013.
- [21] R. Tamassia, G. D. Battista, and C. Batini. Automatic graph drawing and readability of diagrams. *IEEE Transactions on Systems, Man, and Cybernetics*, 18:61–79, 1988.
- [22] L. G. Valiant. Universality considerations in VLSI circuits. *IEEE Transactions on Computers*, 30(2):135–140, 1981.